# Chapter 26

# Cumulus Processes and the Composition of Magmatic Ore Deposits: Examples from the Talnakh District, Russia

M.L. Zientek[1], A.P. Likhachev[2], V.E. Kunilov[3], S.-J. Barnes[4], A.L. Meier[5], R.R. Carlson[5], P.H. Briggs[5], T.L. Fries[6] and B.M. Adrian[5]

[1]U.S. Geological Survey, W.904 Riverside Ave., Spokane, Washington, 99201–1087

[2]Central Research Institute of Geological Prospecting for Base and Precious Metals, Varshavskoye Sh.129B, Moscow 113545, Russia

[3]Norilsky GMK, 2, Gvardeyskaya sc., Noril'sk 663300, Russia

[4]Science de la Terre, Universite du Quebec, Chicoutimi, G7H 2B1

[5]U.S. Geological Survey, Box 25046 Denver Federal Center, Denver, Colorado, 80225–0046

[6]U.S. Geological Survey, 345 Middlefield Road, Menlo Park, California, 99025

## Abstract

**A remarkable feature of the Noril'sk–Talnakh area is the mineralogical and compositional zonation of the magmatic sulphide ore deposits. This zonation can be explained by fractional crystallization of sulphide liquid. The compositions of analyzed ore samples can be identified as belonging to a continuum ranging from evolved, residual liquids derived during the fractionation process to cumulates composed primarily of monosulphide solid solution with variable proportions of trapped liquid.**

**Some massive-ore samples display chondrite-normalized platinum group element-gold patterns with negative platinum anomalies. This feature indicates that the dominant control on ore composition is not sulphide liquid-silicate liquid partitioning but is the composition of monosulphide solid solution derived from the crystallization of sulphide liquid. Massive-sulphide ores that have compositional features typical of sulphide cumulates are not limited to the Noril'sk–Talnakh area but occur in several districts in a range of geological settings.**

## INTRODUCTION

The copper-nickel-platinum group element deposits of the Noril'sk–Talnakh area occur in relatively small, hypabyssal, differentiated mafic intrusions that are temporally and spatially related to the Mesozoic Siberian continental flood basalt province. Resource information about these deposits is difficult to obtain, but available data suggest that they contain in excess of 20 million metric tons of copper and nickel (metal), comparable to the Sudbury district in Canada (DeYoung et al. 1985). Ninety percent of the nickel, 50% of the copper, 75% of the cobalt and virtually all of the platinum-group elements (PGE) produced in Russia come from these deposits (V.E. Kunilov, Norilsky GMK, personal communication, 1992). The Noril'sk–Talnakh deposits thus represent the largest known repository of PGE outside the Bushveld Complex in South Africa (Naldrett 1989). In the recent past, PGE production from the former Soviet Union was thought to be roughly equivalent to the output from South Africa (Coombes 1991).

Mineralogical zonation that occurs from centimetre-sized globules to major orebodies is one of the striking features of the sulphide accumulations. Ellipsoidal aggregates of sulphide minerals from 0.5 to 3 cm in diameter, characteristic of disseminated ores in taxitic and picritic rocks, are sharply divided into 2 domains—1 rich in copper-iron sulphide minerals at the top of the droplet and 1 rich in pyrrhotite and pentlandite at the bottom (*see* Figure 5 in Czamanske et al. 1992). Massive orebodies are characterized by systematic changes in the proportions and abundance of minerals that occur on the scale of hundreds of metres to kilometres.

This mineralogical zonation corresponds to pronounced compositional changes that can largely be attributed to fractionation of monosulphide solid solution (MSS) from sulphide liquids. This paper will focus on how ore compositions have been affected by fractional crystallization of MSS and how the compositional affects of this process can be recognized in deposits elsewhere.

## GEOLOGICAL SETTING AND CHARACTERISTICS OF THE ORE

The ore deposits of the Noril'sk–Talnakh area are associated with hypabyssal intrusions associated with the Siberian flood basalt province. Milanovskiy (1976) estimates that rocks associated with early Mesozoic flood basalt magmatism covered an area of $4 \times 10^6$ km$^2$ in the whole of middle northern Eurasia and had a volume of $2 \times 10^6$ km$^3$. In addition to the better known exposures on the Siberian Platform, flood basalts and related rocks are also found in the late Mesozoic fold and thrust belt in the Taimyr Peninsula and occur in the basement in widespread localities beneath the western Siberian lowlands (Zonenshain et al. 1990). Plate tectonic reconstructions presented by Zonenshain et al.

(1990) indicate that the eruption of flood basalts occurred in the hinterland of the Uralian fold-thrust belt.

The pattern of rock types in the Noril'sk–Talnakh area (Figure 26.1) has been interpreted as depressions associated with rift structures related to traces of deep faults (Duzhikov et al. 1992) or as folds (Smirnov 1966). The Noril'sk–Kharayelakh fault forms a prominent linear feature on both topographic and magnetic maps for 80 to 100 km and is roughly coincident with the axis of the synformal structures that constitute the Noril'sk and Kharayelakh basins. Intrusions that host the ore deposits of the Noril'sk–Talnakh area occur near this fault.

The ore deposits are associated with a specific type of intrusion within the sill complex that formed at the time of

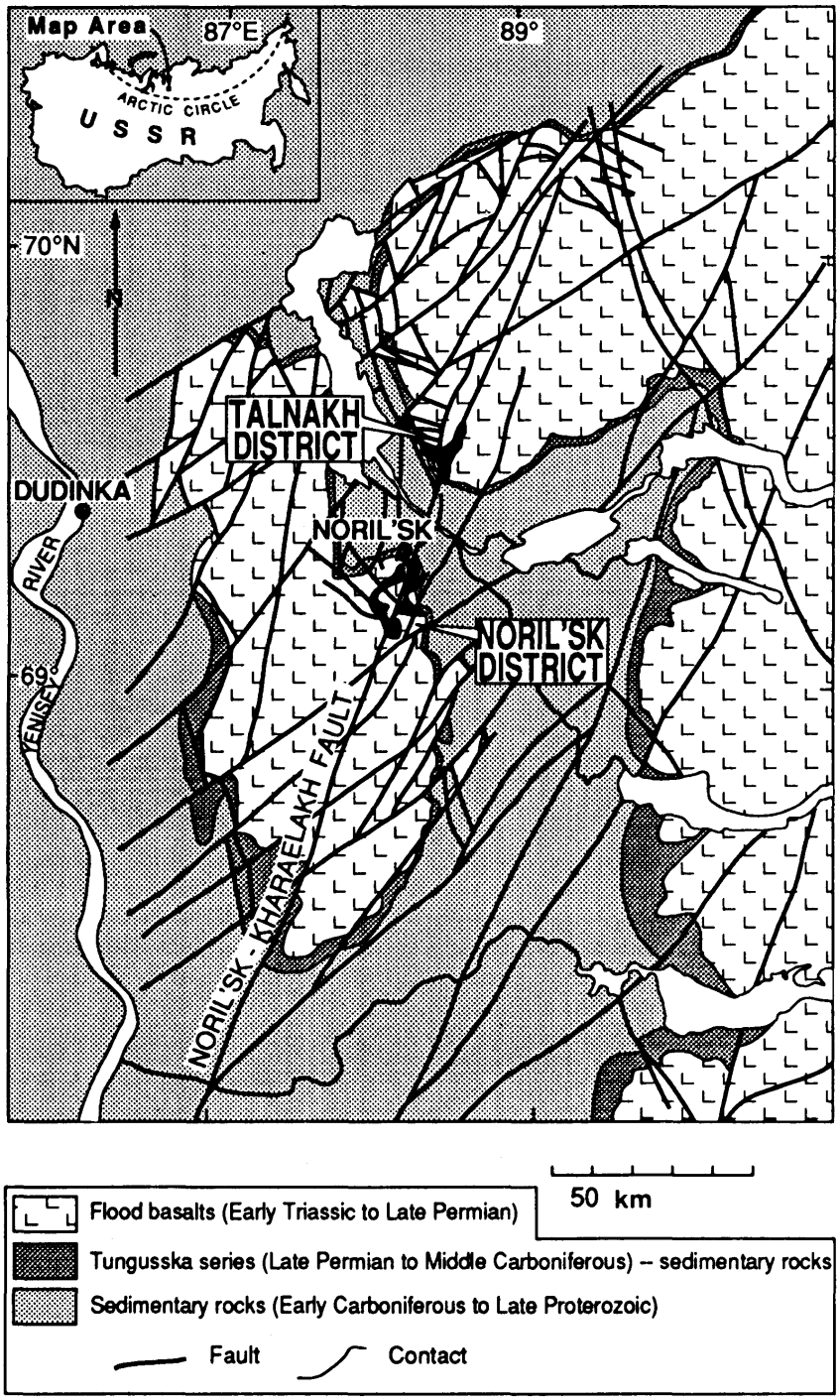


**Figure 26.1.** Simplified geological map of the Noril'sk–Talnakh area showing subsurface outlines of the fully differentiated, ore-bearing intrusions (black).

flood basalt magmatism. The so-called ore-bearing intrusions are "fully" differentiated, elongate, "finger-like" domains that are part of more laterally extensive, less-differentiated sheet-like sills that are tens of metres thick (Smirnov 1966; Zen'ko and Czamanske, this volume). The inflated, finger-like parts of the sills typically can be as much as 350 m thick and 2.5 km wide and have lengths on the order of tens of kilometres. Outlines of the ore-bearing intrusions typically show only the extent of the fully differentiated, finger-like lobes of the sills (Figure 26.2). Where hosted by sedimentary rocks, these elongate, ore-bearing intrusions are surrounded by metamorphic and metasomatic aureoles that are larger than what would be expected for the size of the intrusion (Genkin et al. 1982).

Within the finger-like parts of the sills, silicate-rich rocks form a vertical sequence that is suggestive of *in situ* differentiation by olivine accumulation near the base of the intrusion. The rocks consist predominantly of plagioclase, olivine and augite; much of the modal variation in the rocks reflects changes in the proportions of olivine and plagioclase. Listed in order of decreasing olivine content, rock types include mela-olivine gabbro, olivine gabbro, leuco-olivine gabbro and leucogabbro (Streckeisen 1973); the local terms applied to this same range of rock compositions are picritic gabbrodolerite, picrite-like gabbrodolerite, olivine and olivine-bearing gabbrodolerite, gabbrodolerite or gabbrodiorite and leucogabbro (Zen'ko and Czamanske, this volume; Czamanske et al., this volume). Chilled, sulphide-poor gabbrodolerite occurs along the lower margins of the intrusions; within a few metres, these rocks grade upwards into a fine- to coarse-grained variable-textured olivine gabbrodolerite that contains disseminated sulphide minerals. This variable-textured gabbrodolerite is characterized by irregular variations in texture, mode and grain size on the scale of hand specimen to outcrop; the unit often contains abundant inclusions of earlier crystallized mafic rocks. Russian geologists refer to this unit as taxitic gabbrodolerite (the adjective may be derived from taxite—a volcanic rock that consists of a mixture of materials of varying texture and structure; Gary et al. 1972). These lower taxitic rocks are overlain by fine- to medium-grained picritic gabbrodolerites. Inclusions of the taxitic rocks are found in the lowermost picritic units; where observed by the senior author, these inclusions range from single crystals to polycrystalline aggregates a few centimetres in diameter to sharply defined, rounded fragments several tens of centimetres in diameter. Concentrations of disseminated sulphide minerals occur in the picritic gabbrodolerites as well. From this point, the proportion of olivine generally decreases upsection through olivine-biotite gabbrodolerite, olivine gabbrodolerite and olivine-bearing gabbrodolerite. The uppermost unit, gabbrodolerite or gabbrodiorite, contains little or no olivine; the rocks near the upper contact of the sills are characterized by variable grain size, intrusion breccias, local domains with pegmatoidal textures and melt segregations. Irregularly, leucogabbro is present at the upper contacts of the intrusions.

However, the ore-bearing intrusions most probably do not form by simple *in situ* differentiation of a single batch of magma, but by emplacement of multiple pulses of magma of differing composition (Czamanske et al., this volume). The transitions between rock types typically do not reflect a gradational change in the proportion of olivine but, rather, are characterized by abrupt changes in mode, grain size and texture. Multiple modally graded sequences may occur in a section, and significant lateral changes in the proportion of rock types are common. An abrupt change in initial strontium isotope ratios across a lithologic transition from picritic gabbrodolerite to olivine gabbrodolerite in drill hole KZ1879 through the Kharayelakh intrusion is the most direct evidence that some of these lithologic changes may result from the repeated influx of magma.

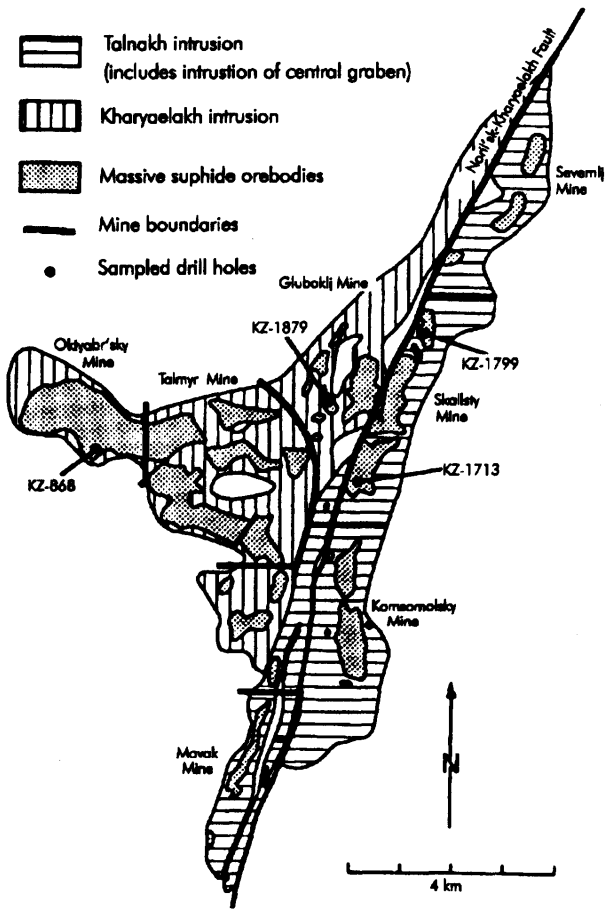


**Figure 26.2.** Plan showing subsurface extent of the ore-bearing branches of the Talnakh and Kharayelakh intrusions, Talnakh district, with locations of massive orebodies, drill hole sites and mine designations.

## Sulphide Mineralization

Depending on the amount of sulphide present and the spatial-temporal relation to intrusive rocks, sulphide mineralization has been subdivided into: 1) disseminated ores in intrusive rocks, 2) massive ores and 3) veinlet-disseminated ores and breccioid ores in country rocks adjacent to the mineralized intrusions (Genkin et al. 1982; Duzhikov et al. 1992). Our sampling has primarily focussed on the first 2 ore types.

Disseminated-sulphide mineralization within the ore-bearing intrusions is typically concentrated in the middle and lower parts of the picritic units and the upper and middle parts of the taxitic units near the lower margin of the intrusions. Away from this interval, the amount of sulphide minerals gradually decreases to the lower contact of the intrusion and decreases in rocks overlying the picritic unit. Morphological types of disseminated sulphide aggregates include ovoid-drop-like forms, which occur principally in the picritic units, and interstitial grains that form irregular shapes moulded against silicate minerals or form thin intergranular films along silicate grain boundaries.

Massive ores vary in their setting, size and distribution. They range from thin veinlets to sheet-like orebodies that can extend for several kilometres with thickness ranging up to 50 m. Although massive ores are spatially associated with the ore-bearing intrusions, they are not a typical end-member of a textural continuum that would include matrix ore and disseminated ore. Massive-sulphide orebodies show sharp and sometimes transgressive contacts with the ore-bearing intrusions; this temporal relation is also supported by a lack of matrix ore in most intrusions and the virtual absence of entrained igneous silicate minerals in massive ores. In the Talnakh district, massive ores are localized in rocks underlying the intrusions and, to a lesser extent, in the lower contact zone of the intrusions. Massive ores in the metamorphosed sedimentary rocks typically have no direct contact with the ore-bearing intrusions. The largest deposits are localized along the axis defining the thickest part of the elongate, ore-bearing intrusions (*see* Figure 26.2). In the Noril'sk district, massive-sulphide veins form an anastomosing zone of sheet-like orebodies that occur in rocks adjacent to the Noril'sk I intrusion, as well as in the lower part of the intrusion near the transition from picritic to taxitic rocks (Smirnov 1966).

Veinlet-disseminated ores form in the contact-metamorphic aureoles of the ore-bearing intrusions and are commonly concentrated in envelopes surrounding massive-sulphide orebodies. Sulphides occur in veins and as metasomatic replacements; textures are complex and reflect the structural fabric of the rock. For example, sulphide minerals can occur along bedding planes in fissile rocks, in amygdule sites in basalts and at porphyroblast sites in some hornfels.

## SAMPLING AND METHODS

The opportunity to visit the district and collect samples in 1990 was part of a broader memorandum of understanding on scientific exchange between the United States (U.S.) Geological Survey and the Ministry of Geology of the USSR. Two weeks were devoted to investigating the magmatic copper-nickel-PGE ore deposits of the Noril'sk–Talnakh area. Material collected from drill holes in the Noril'sk and Talnakh districts was supplemented by samples collected from the Medvezhy Creek open pit, underground workings of the Oktyabr'sky Mine and ore stockpiles for the Oktyabr'sky and Komsomolsky mines.

Most analyses were carried out in laboratories of the U.S. Geological Survey (Tables 26.1, 26.2, 26.3 and 26.4). Analytical methods are as follows: iron, nickel, copper, silver, cobalt, lead and zinc by inductively coupled plasma atomic emission spectrometry (ICP–AES) (Lichte et al. 1987); sulphur by combustion with infrared (IR) detection (Jackson et al. 1987); arsenic and antimony by hydride-generation atomic absorption spectrometry (AAS); tellurium and bismuth by ion-exchange plus graphite-furnace

**Table 26.1.** Representative analytical data for massive-sulphide ores, Oktyabr'sk Mine area, western branch of Kharayelakh intrusion; mineral assemblages are listed in decreasing order of abundance.

| Sample Number | Mineral assemblage | Fe, wt. % | Cu, wt. % | Ni, wt. % | S, wt. % | Ir, ppb | Ru, ppb | Rh, ppb | Pt, ppb | Pd, ppb | Au, ppm |
|---|---|---|---|---|---|---|---|---|---|---|---|
| KZ868 892.4 | po–cp–pn | 45.0 | 1.80 | 2.75 | 27.8 | 7.8 | 14 | 120 | 630 | 3 570 | 0.10 |
| 90OMZS2–3* | po–cp–pn | 54.7 | 4.05 | 3.48 | 30.5 | 20 | 57 | 240 | 1,600 | 10 800 | 0.05 |
| 90OC4* | cp–po–pn | 47.3 | 12.30 | 3.03 | 32.4 | 6 | 18 | 85 | 4,190 | 21 300 | 0.93 |
| 90OMZS1–4 | cp–po–pn | 51.2 | 10.30 | 2.88 | 29.0 | 44 | 89 | 450 | 6,150 | 20 000 | 0.70 |
| 900MZS1–3* | cp–po–cb–pn | 39.8 | 22.80 | 2.13 | 32.9 | 44 | 96 | 290 | 7,500 | 29 100 | 1.40 |
| 90OC13* | cp–po–cb–pn | 41.1 | 20.80 | 1.80 | 32.9 | 4.1 | 15 | 33 | 2,600 | 37 000 | 1.10 |
| 90OMZS1–1* | mh–tk–pn | 35.6 | 28.30 | 2.48 | 31.3 | 1.4 | <5 | 26 | 23,000 | 77 000 | 5.30 |
| 90OC9* | mh–tk–pn | 37.0 | 27.20 | 2.61 | 30.1 | <0.5 | <5 | 10 | 21,000 | 119 000 | 3.97 |
| 90OC14* | mh–tk–pn | 34.5 | 28.00 | 3.49 | 33.5 | 0.9 | <5 | 14 | 20,500 | 140 000 | 1.05 |
| 90OC8 | cp–pn | 35.3 | 29.30 | 1.87 | 31.7 | <5 | <5 | 9.0 | 4,500 | 39 000 | 2.35 |
| 90OMZ67–5–1* | cp–pn | 30.6 | 31.10 | 2.56 | 33.1 | 0.6 | <5 | 3.6 | 1,900 | 28 000 | 0.28 |

*Mineral abbreviations: po–pyrrhotite, cp–chalcopyrite, cb–cubanite, mh–mooihoekite, tk–talnakhite, and pn–pentlandite. Minerals in assemblage name are listed in decreasing order of abundance.*

*Fe, Cu, and Ni by ICP–AES (P.H. Briggs, U.S. Geological Survey, Denver), S by combustion and IR detection (T.L. Fries, U.S. Geological Survey, Menlo Park); Au by graphite furnace AA (B.M. Adrian, U.S. Geological Survey, Denver). See text for additional information. Notes apply to Tables 2, 3, and 4.*

Values reported for Fe, Cu, Ni and S are the mean of replicate analyses. PGE and Au concentrations are the median value.

**PGE by NiS fire assay and ICP–MS and INAA (A.L. Meier and R.R Carlson, U.S. Geological Survey, Denver and S.–J. Barnes, University of Quebec, Chicoutimi).*

**Table 26.2.** Analytical data for drill hole KZ868, Oktyabr'sky Mine area, western branch of Kharayelakh intrusion.

| Sample Number | Rock Type | Ore Type | Fe, wt. % | Cu, wt. % | Ni, wt. % | S, wt. % | Ir, ppb | Ru, ppb | Rh, ppb | Pt, ppb | Pd, ppb | Au, ppm |
|---|---|---|---|---|---|---|---|---|---|---|---|---|
| KZ868 842.7 | picritic gabbrodolerite | disseminated | 7.10 | 0.10 | 0.06 | 0.63 | 1.5 | 4.7 | 7.9 | 76 | 200 | — |
| KZ868 858.1 | taxitic gabbrodolerite | disseminated | 10.0 | 0.47 | 0.23 | 2.66 | 3.9 | 11 | 28 | 220 | 910 | — |
| KZ868 860.2 | taxitic gabbrodolerite | disseminated | 9.70 | 0.31 | 0.17 | 1.79 | 2.2 | 7.2 | 18 | 140 | 540 | — |
| KZ868 863.8 | taxitic gabbrodolerite | matrix | 13.0 | 1.60 | 0.46 | 5.26 | 6.2 | 21 | 47 | 790 | 2 800 | — |
| KZ868 868.3 | taxitic gabbrodolerite | disseminated | 10.0 | 0.55 | 0.25 | 3.11 | 4.8 | 15 | 34 | 310 | 1 000 | — |
| KZ868 879.5 | taxitic gabbrodolerite | matrix | 15.0 | 2.00 | 0.49 | 6.23 | 3.8 | 12 | 35 | 1 100 | 3 400 | — |
| KZ868 883.8 | taxitic gabbrodolerite | matrix | 15.0 | 1.90 | 0.67 | 6.22 | 7.8 | 19 | 64 | 1 270 | 4 070 | 0.30 |
| KZ868 890 | taxitic gabbrodolerite | disseminated | 11.0 | 0.40 | 0.18 | 1.96 | 2.7 | 8.7 | 22 | 150 | 940 | — |
| KZ868 890* | taxitic gabbrodolerite | disseminated | 11.0 | 0.40 | 0.18 | 2.00 | 2.7 | 8.8 | 22 | 170 | 880 | — |
| KZ868 892.4 | massive sulphide | massive | 45.0 | 1.80 | 2.75 | 27.8 | 7.8 | 14 | 120 | 630 | 3 570 | 0.10 |
| KZ868 898* | massive sulphide | massive | 49.3 | 2.67 | 3.54 | 34.4 | 7.3 | 11 | 130 | 790 | 4 250 | 0.10 |
| KZ868 898.4* | Cu–rich sulphide segregations in hornfels | matrix | 13.0 | 4.00 | 0.84 | 7.40 | 0.3 | <0.5 | 4.3 | 2 300 | 9 100 | 0.50 |
| KZ868 899.1 | massive sulphide | massive | 49.7 | 2.90 | 3.15 | 30.8 | 3.5 | 4.7 | 87 | 1 800 | 6 400 | 0.13 |
| KZ868 901.5 | massive sulphide | massive | 46.0 | 2.70 | 2.97 | 30.5 | 8.1 | 21 | 130 | 810 | 4 270 | 0.05 |
| KZ868 903.1 | massive sulphide | massive | 49.0 | 2.57 | 3.01 | 29.2 | 7.7 | 14 | 110 | 870 | 4 600 | <0.05 |
| KZ868 907.5 | massive sulphide | massive | 52.0 | 4.50 | 3.74 | 35.2 | 42 | 95 | 400 | 2 170 | 8 830 | 0.20 |
| KZ868 908.5 | massive sulphide | massive | 50.7 | 3.60 | 3.39 | 31.1 | 27 | 57 | 330 | 1 800 | 8 370 | 0.18 |
| KZ868 911.4 | massive sulphide | massive | 49.0 | 4.27 | 3.39 | 31.4 | 22 | 29 | 310 | 1 470 | 7 670 | 0.12 |
| KZ868 912.6 | massive sulphide | massive | 40.0 | 3.97 | 2.21 | 20.8 | 12 | 20 | 167 | 1 100 | 5 230 | 0.15 |
| KZ868 914 | massive sulphide | massive | 51.7 | 5.23 | 4.01 | 36.6 | 41 | 110 | 410 | 2 130 | 10 300 | 0.20 |
| KZ868 914.9* | massive sulphide | massive | 51.7 | 5.30 | 3.75 | 35.5 | 42 | 120 | 410 | 1 950 | 10 000 | 0.15 |
| KZ868 918 | massive sulphide | massive | 53.0 | 4.70 | 3.73 | 34.4 | 38 | 100 | 430 | 1 830 | 10 000 | 0.10 |
| KZ868 919 | massive sulphide | massive | 43.7 | 4.27 | 2.08 | 21.1 | 14 | 17 | 187 | 1 700 | 6 370 | 0.10 |
| KZ868 920.8* | massive sulphide | massive | 50.0 | 5.37 | 3.66 | 33.7 | 14 | 22 | 190 | 2 550 | 11 000 | 0.20 |
| KZ868 923 | massive sulphide | massive | 50.0 | 5.00 | 2.64 | 24.5 | 14 | 28 | 140 | 2 100 | 9 330 | 0.22 |

*Mineral abbreviations are: po–pyrrhotite, cp–chalcopyrite, cb–cubanite, mh–mooihoekite, tk–talnakhite, and pn–pentlandite. Minerals in assemblage name are listed in decreasing order of abundance.*

*Fe, Cu, and Ni by ICP–AES (P.H. Briggs, U.S. Geological Survey, Denver), S by combustion and IR detection (T.L. Fries, U.S. Geological Survey, Menlo Park); Au by graphite furnace AA (B.M. Adrian, U.S. Geological Survey, Denver). See text for additional information. Notes apply to Tables 2, 3, and 4.*

Values reported for Fe, Cu, Ni and S are the mean of replicate analyses. PGE and Au concentrations are the median value.

**PGE by NiS fire assay and ICP–MS and INAA (A.L. Meier and R.R Carlson, U.S. Geological Survey, Denver and S.–J. Barnes, University of Quebec, Chicoutimi).*

**Table 26.3.** Analytical data for drill hole KZ1879, Glubokij Mine area, northern branch of Kharayelakh intrusion.

| Sample Number | Rock Type | Ore Type | Fe, wt. % | Cu, wt. % | Ni, wt. % | S, wt. % | Ir, ppb | Ru, ppb | Rh, ppb | Pt, ppb | Pd, ppb | Au, ppm |
|---|---|---|---|---|---|---|---|---|---|---|---|---|
| KZ1879 1752.5 | picritic gabbrodolerite | disseminated | 13.0 | 0.96 | 0.53 | 2.90 | 12 | 36 | 100 | 810 | 2 900 | 0.20 |
| KZ1879 1757 | picritic gabbrodolerite | disseminated | 12.0 | 0.50 | 0.36 | 1.59 | 6.5 | 19 | 58 | 410 | 1 500 | 0.10 |
| KZ1879 1761.0 | picritic gabbrodolerite | disseminated | 12.0 | 0.48 | 0.33 | 1.32 | 6.5 | 21 | 68 | 550 | 1 900 | 0.15 |
| KZ1879 1763.1 | picritic gabbrodolerite | disseminated | 11.0 | 0.41 | 0.30 | 1.22 | 4.5 | 14 | 48 | 430 | 1 600 | 0.10 |
| KZ1879 1767.9 | picritic gabbrodolerite | disseminated | 11.0 | 0.33 | 0.24 | 0.95 | 3.7 | 11 | 37 | 280 | 1 100 | 0.15 |
| KZ1879 1768.5B | picritic gabbrodolerite | disseminated | 10.0 | 0.66 | 0.33 | 2.08 | 5.3 | 19 | 55 | 380 | 1 700 | — |
| KZ1879 1773.0 | picritic gabbrodolerite | disseminated | 9.10 | 0.45 | 0.20 | 1.33 | 2.1 | 8.4 | 40 | 220 | 890 | — |
| KZ1879 1777.4 | picritic gabbrodolerite | disseminated | 11.0 | 0.43 | 0.23 | 1.12 | 4.3 | 14 | 39 | 250 | 1 100 | — |
| KZ1879 1785.5 | taxitic gabbrodolerite | disseminated | 11.0 | 0.64 | 0.27 | 2.19 | 4.8 | 18 | 48 | 310 | 1 300 | — |
| KZ1879 1791.6 | taxitic gabbrodolerite | matrix | 11.0 | 1.20 | 0.75 | 4.49 | 13 | 33 | 140 | 1 200 | 3 300 | 0.15 |
| KZ1879 1800.2* | massive sulphide | massive | 49.7 | 6.67 | 4.59 | 35.4 | 210 | 700 | 1 610 | 2 200 | 11 500 | 0.15 |
| KZ1879 1802.5 | massive sulphide | massive | 52.0 | 4.57 | 4.47 | 31.5 | 61 | 130 | 740 | 2 600 | 12 000 | 0.10 |
| KZ1879 1805 | massive sulphide | massive | 50.0 | 6.70 | 4.71 | 35.4 | 170 | 490 | 1 300 | 2 670 | 12 000 | 0.17 |
| KZ1879 1807.7* | massive sulphide | massive | 52.7 | 4.00 | 4.74 | 32.6 | 27 | 92 | 330 | 1 600 | 9 450 | 0.07 |
| KZ1879 1808 | massive sulphide | massive | 52.0 | 3.27 | 5.13 | 34.3 | 28 | 74 | 350 | 2 130 | 11 700 | 0.05 |

*Mineral abbreviations are: po–pyrrhotite, cp–chalcopyrite, cb–cubanite, mh–mooihoekite, tk–talnakhite, and pn–pentlandite. Minerals in assemblage name are listed in decreasing order of abundance.*

*Fe, Cu, and Ni by ICP–AES (P.H. Briggs, U.S. Geological Survey, Denver), S by combustion and IR detection (T.L. Fries, U.S. Geological Survey, Menlo Park); Au by graphite furnace AA (B.M. Adrian, U.S. Geological Survey, Denver). See text for additional information. Notes apply to Tables 2, 3, and 4.*

Values reported for Fe, Cu, Ni and S are the mean of replicate analyses. PGE and Au concentrations are the median value.

**PGE by NiS fire assay and ICP–MS and INAA (A.L. Meier and R.R Carlson, U.S. Geological Survey, Denver and S.–J. Barnes, University of Quebec, Chicoutimi).*

AAS; and tin by solvent extraction plus graphite-furnace AAS (Wilson et al. 1987; Zientek et al. 1990; Aruscavage and Crock 1987). Platinum group elements were determined by NiS fire assay and inductively coupled plasma mass spectrometry (ICP–MS) in 10 g samples at limits of 0.5 ppb or lower (Meier et al. 1991). The method used is similar to the procedures described by Robert et al. (1971) and Jackson et al. (1990). Without modification, the useful range of the method is from the detection limit to about 5 ppm; for samples of PGE-enriched copper-rich ore, the sample size was reduced to 2 g or less. Accuracy is improved by isotope dilution using enriched $^{191}Ir$ to track recovery through the collection and separation procedure. Analytical results were referenced against SARM–7; the precision obtained for 60 replicate analyses of 1 g samples of SARM–7 analyzed with routine samples over a 6 month period is as follows (expressed as relative standard deviation): ruthenium, 8.34%; rhodium, 5.41%; palladium, 6.29%; iridium, 8.90%; and platinum, 6.60%. Replicate analyses were performed for all ore samples: at least 2 for disseminated-ore samples; 3 or more for massive ore samples. Because there was some question about the necessity and affect of corrections in the determinations of rhodium and ruthenium, 30 samples that span the compositional range of the massive-sulphide ores were selected and analyzed by NiS fire assay and instrumental neutron activation (INAA) at the University of Quebec at Chicoutimi. Results for rhodium, platinum and gold generally agree (the average of differences is less than 2%). Although there can be substantial differences in the concentrations of these elements among samples, there is no systematic bias between laboratories. Results for iridium were also in

**Table 26.4.** Analytical data for drill holes KZ1713 and KZ1799, Skalisty Mine area, Talnakh intrusion.

| Sample Number | Rock Type | Ore Type | Fe, wt. % | Cu, wt. % | Ni, wt. % | S, wt. % | Ir, ppb | Ru, ppb | Rh, ppb | Pt, ppb | Pd, ppb | Au, ppm |
|---|---|---|---|---|---|---|---|---|---|---|---|---|
| KZ1713 862.8 | olivine–gabbrodolerite | disseminated | 6.80 | 0.03 | 0.03 | 0.13 | 0.6 | 2.0 | 10 | 59 | 190 | — |
| KZ1713 883.8 | olivine–gabbrodolerite | disseminated | 16.0 | 0.57 | 0.40 | 1.88 | 15 | 40 | 110 | 790 | 2 200 | 0.10 |
| KZ1713 886.5 | olivine–gabbrodolerite | disseminated | 7:60 | 0.15 | 0.09 | 0.56 | 3.0 | 9.2 | 28 | 190 | 510 | — |
| KZ1713 902.8 | olivine–gabbrodolerite | matrix | 14.0 | 1.40 | 0.83 | 5.60 | 21 | 63 | 190 | 1 100 | 3 500 | 0.20 |
| KZ1713 910.5 | picritic gabbrodolerite | matrix | 14.0 | 0.87 | 0.68 | 4.09 | 18 | 54 | 160 | 750 | 2 800 | 0.10 |
| KZ1713 922.9 | taxitic gabbrodolerite | matrix | 13.0 | 1.70 | 0.65 | 4.66 | 11 | 36 | 120 | 670 | 5 200 | 0.35 |
| KZ1713 928.1 | massive sulphide | massive | 48.0 | 1.93 | 3.79 | 22.6 | 180 | 430 | 1 800 | 940 | 5 170 | 0.10 |
| KZ1713 931.3* | massive sulphide | massive | 52.0 | 2.50 | 5.53 | 37.0 | 780 | 3 250 | 5 050 | 1 240 | 6 550 | 0.10 |
| KZ1713 934.6 | massive sulphide | massive | 50.7 | 4.97 | 4.89 | 36.5 | 670 | 3 100 | 4 500 | 1 170 | 6 100 | 0.15 |
| KZ1799 1321.55 | picritic olivine–gabbrodolerite | disseminated | 9.50 | 0.52 | 0.28 | 1.22 | 6.7 | 19 | 46 | 370 | 1 200 | 0.10 |
| KZ1799 1338.5 | taxitic gabbrodolerite | matrix | 14.0 | 1.97 | 1.06 | 6.88 | 25 | 68 | 220 | 1 530 | 6 400 | 0.35 |
| KZ1799 1343 | hornfels | massive | 26.7 | 2.00 | 2.54 | 17.8 | 240 | 800 | 1 570 | 740 | 4 030 | 0.10 |
| KZ1799 1347.9 | massive sulphide | massive | 45.0 | 2.50 | 4.12 | 28.4 | 25 | 25 | 600 | 950 | 5 300 | 0.07 |
| KZ1799 1351 | massive sulphide | massive | 37.0 | 2.50 | 3.25 | 22.0 | 100 | 230 | 1 100 | 1 600 | 6 200 | 0.10 |

*Mineral abbreviations are: po–pyrrhotite, cp–chalcopyrite, cb–cubanite, mh–mooihoekite, tk–talnakhite, and pn–pentlandite. Minerals in assemblage name are listed in decreasing order of abundance.*

*Fe, Cu, and Ni by ICP–AES (P.H. Briggs, U.S. Geological Survey, Denver), S by combustion and IR detection (T.L. Fries, U.S. Geological Survey, Menlo Park); Au by graphite furnace AA (B.M. Adrian, U.S. Geological Survey, Denver). See text for additional information. Notes apply to Tables 2, 3, and 4.*

Values reported for Fe, Cu, Ni and S are the mean of replicate analyses. PGE and Au concentrations are the median value.

**PGE by NiS fire assay and ICP–MS and INAA (A.L. Meier and R.R Carlson, U.S. Geological Survey, Denver and S.–J. Barnes, University of Quebec, Chicoutimi).*

agreement except for very copper-rich samples where the results of the ICP-MS analyses were higher. The reason for the difference is not known; there are no obvious interferences that should affect the ICP-MS or the INAA results. However, because sample weights had to be reduced for these high copper samples, the results reported by ICP-MS were close to the determination limit and are more likely to be in error. Determinations of palladium by ICP-MS were consistently lower than the results obtained by INAA (by an average difference of 14%). Both laboratories reference their analyses to the same standard, SARM–7, but the concentration of palladium in the ore samples was in almost all cases greater than the standard (by as much 2 orders of magnitude). The difference has not been reconciled largely due to the lack of appropriate standard material with high concentrations of PGE. Because of interference problems in the INAA method, the ICP-MS method gave a better indication of the ruthenium contents of ore samples with high concentrations of gold and copper.

# RESULTS

## Mineralogical and Compositional Zonation of Massive Ores—Oktyabr'sky Mine

Genkin et al. (1982) distinguish 2 patterns of zonation in massive ores of the Noril'sk–Talnakh area, simple and complex. Simple zonation refers to a change from

pyrrhotite-dominant ores to chalcopyrite-dominant ores by gradual changes in proportions of pyrrhotite and chalcopyrite. Ores enriched in chalcopyrite are typically concentrated at the margins of orebodies. Complex zonation refers to the succession of numerous mineral varieties of ore that include zones enriched in cubanite or mooihoekite (talnakhite), as well as pyrrhotite and chalcopyrite.

The massive-sulphide ores of the Oktyabr'sky Mines area display a concentric arrangement of ore types with various proportions of sulphide minerals typical of complex zonation (Figure 26.3). Mineral assemblages at the outer, lateral edges and lower margins of the orebody are pyrrhotite-rich with lesser amounts of chalcopyrite and pentlandite. Inwards, successive zones of chalcopyrite-dominant and cubanite-dominant assemblages surround a core of mooihoekite-cubanite or talnakhite-cubanite assemblages in the central and upper parts of the deposit. All assemblages carry pentlandite.

Genkin et al. (1982) and Stekhin (1992) both note that the complexly zoned massive ores of the Oktyabr'sky Mine occur at the western end of the main Kharayelakh orebody, which extends from the Oktyabr'sky Mine into the Taimyr Mine area and is likely continuous with the massive orebody at the southern margin of the Taimyr Mine area (*see* Figure 26.2). Throughout most of their length, the main Kharayelakh orebody and the adjacent orebody in the Taimry Mine are made up of pyrrhotite-dominant massive-sulphide ores characterized by simple zoning. These orebodies are localized along an axial zone of the finger-like intrusion that composes the southern margin of the western branch of the Kharayelakh intrusion (Duzhikov et al. 1992).

The mineralogical zonation corresponds to compositional zonation (*see* Table 26.1). In Figure 26.4, data for samples collected from pyrrhotite-chalcopyrite and chalcopyrite-pyrrhotite assemblages (pyrrhotite-rich ores; Cu/S less than 0.4) from the outer parts of the zonation sequence

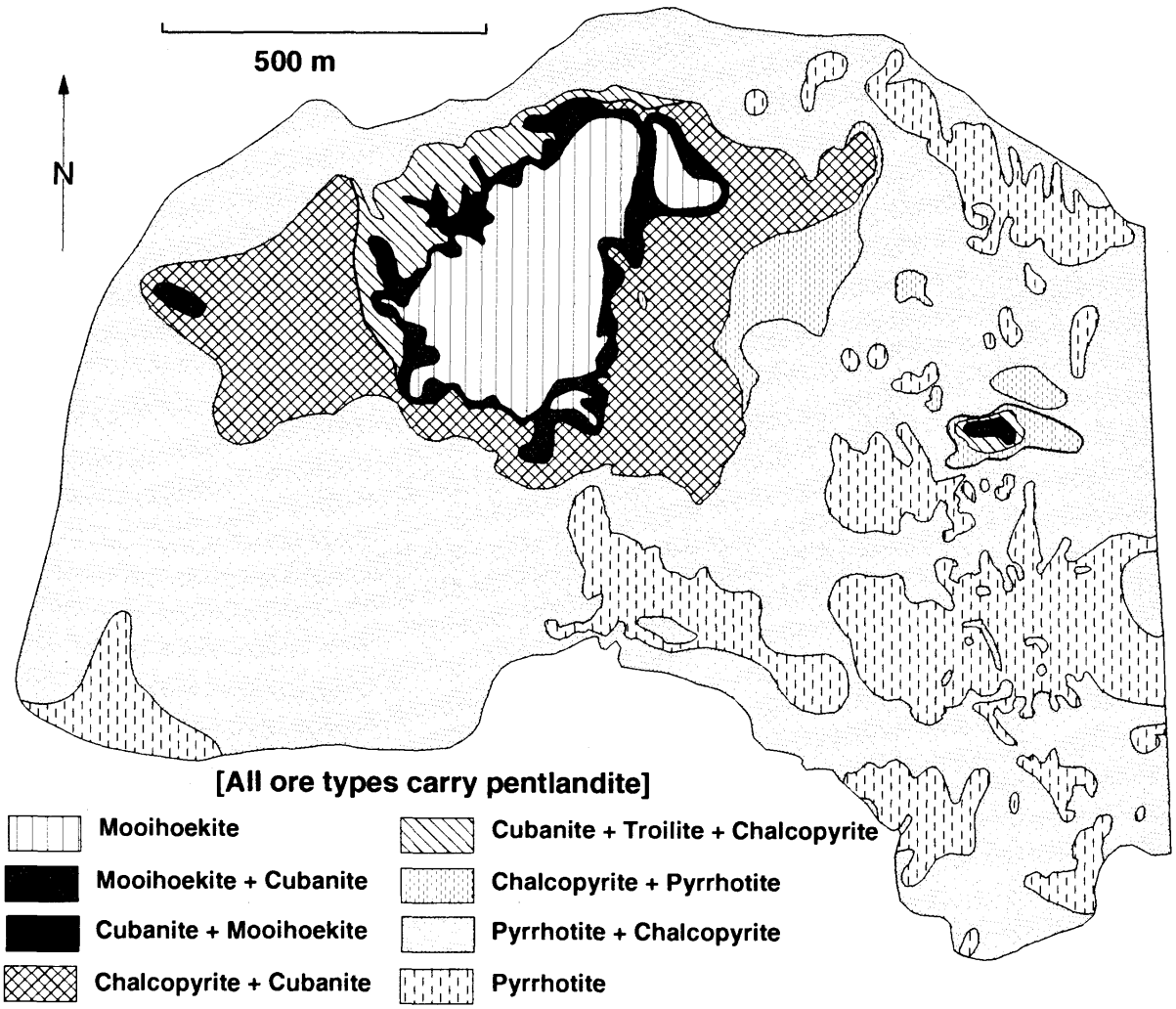


**Figure 26.3.** Plan map of mineral-assemblage zonation in massive-sulphide ores in the Oktyabr'sky Mine area, western branch of the Kharayelakh intrusion.

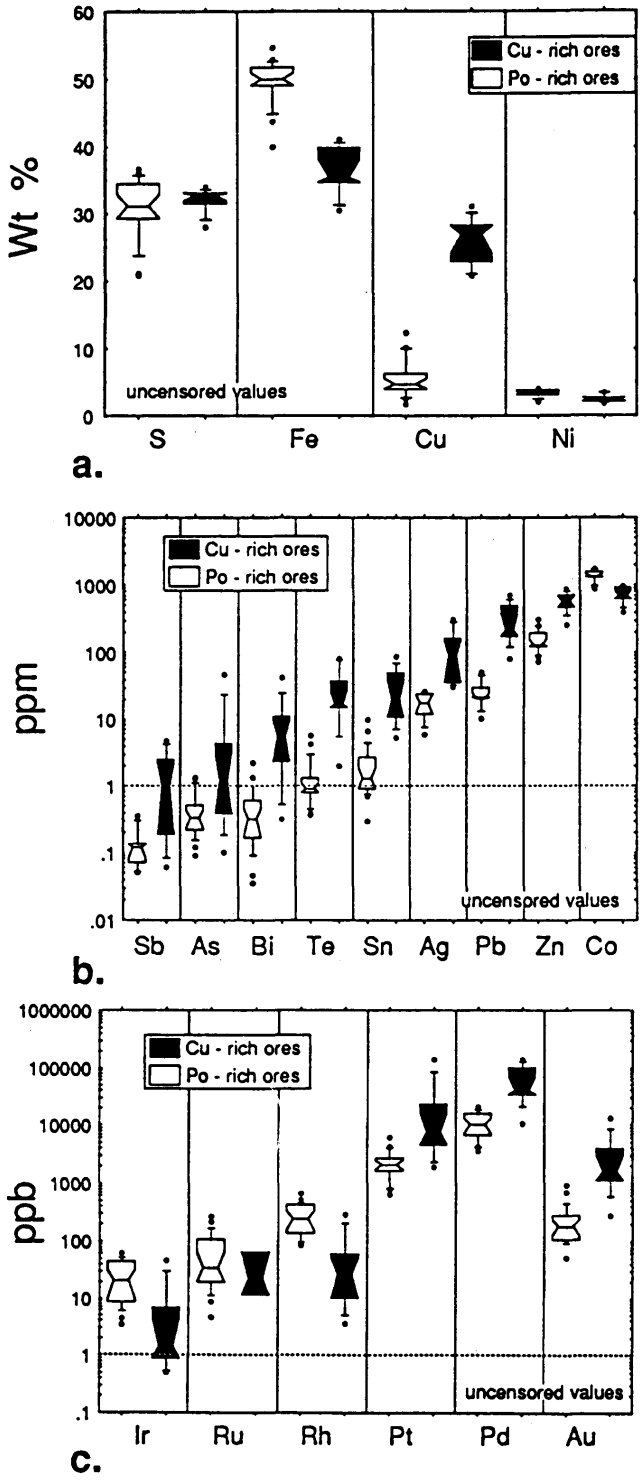


**Figure 26.4.** Box-and-whisker plots illustrating major and minor element concentrations in massive-sulphide ores of the Oktyabr'sky Mine area. **a)** S, Fe, Cu and Ni; **b)** Sb, As, Bi, Te, Sn, Ag, Pb, Zn and Co; and **c)** Ir, Ru, Rh, Pt, Pd and Au. Key to symbols: horizontal line in box is the median value of the data; ends of the boxes are the 25th and 75th percentiles of the data; lines at ends of boxes ("whiskers") extend to the 10th and 90th percentiles of the data; and dots on the top and bottom of the lines show outlier points of data distribution. Notches on the sides of the boxes show the 90th percent confidence interval about the median value. Po–pyrrhotite.

in the Oktyabr'sky Mine area are compared to samples from the mooihoekite- and talnakhite-bearing assemblages (copper-rich ores; Cu/S greater than 0.6) in the core of the deposit. Compositional differences between the 2 groups of samples are entirely consistent with what is known experimentally about the partitioning behavior of elements between sulphide liquid and MSS (Craig and Kullerud 1969; Distler et al. 1977; Fleet et al. 1992; M.E. Fleet, University of Western Ontario, personal communication, 1992). Samples rich in copper are enriched in elements known to behave incompatibly during MSS crystallization: copper, platinum, palladium and gold (*see* Figure 26.4a). Pyrrhotite-rich samples are enriched in elements known to behave compatibly: iron, nickel, cobalt, iridium, ruthenium and rhodium (*see* Figures 26.4b and 26.4c). By analogy, the data presented in Figure 26.4b suggest that antimony, arsenic, bismuth, tellurium, tin, silver, lead and zinc behave incompatibly during MSS fractionation. Chondrite-normalized copper-nickel-PGE-gold plots for samples representative of particular assemblages are shown in Figure 26.5. As expected, ratios of incompatible to compatible elements increase from pyrrhotite-bearing to the copper-rich assemblages. Concentrations of platinum, palladium and gold decrease, and copper contents increase slightly between mooihoekite-talnakhite-cubanite-pentlandite assemblages, typical of the core of the mineralogically zoned massive-sulphide orebody, and chalcopyrite-pentlandite assemblages that occur as discordant segregations of massive sulphide that cut the intrusion immediately above the copper-rich massive sulphides. Chalcopyrite-pentlandite ores also contain lower concentrations of antimony, arsenic, bismuth, silver and tellurium, relative to mooihoekite-talnakhite-cubanite-pentlandite ores. If the chalcopyrite-pentlandite ore samples are related to and derived from the underlying massive-sulphide orebody, their compositional characteristics cannot result from MSS fractionation alone; crystallization of other phases such as intermediate solid solution or platinum group minerals from the copper-rich residual liquid must be considered in order to explain the depletion of selected incompatible elements.

Previous reports with data on the composition of ores from Noril'sk–Talnakh area gave no information about the copper-rich ores at Oktyabr'sky. Strishkov (1984) reported that the Oktyabr'sky reserves were 130 million tons of ore containing 3.9 weight % copper (comparable to the copper concentrations in the pyrrhotite-bearing ore assemblages) and gave no indication of the very high copper concentrations in the copper-rich ore (greater than 20 weight %). Previously estimates of the total PGE contents of massive ores were as high as 11 ppm (Hulbert et al. 1988; Wyllie 1987); we know now that PGE concentrations in copper-rich ore are more typically on the order of hundreds of ppm.

## Comparison of Disseminated- and Massive-Ore Compositions

During the course of our investigations, we had the opportunity to sample core from drill holes in the Talnakh district that contained both disseminated ore in picritic and taxitic

units and massive-sulphide ore. The holes included KZ868 in the Oktyabr'sky Mine area in the western branch of the Kharayelakh intrusion (*see* Table 26.2), KZ1879 in the area of the proposed Glubokij Mine in the northern branch of the Kharayelakh intrusion (*see* Table 26.3) and KZ1713 and KZ1799 in the area of the proposed Skalisty Mine in the Talnakh intrusion (*see* Table 26.4). The lithologic sequence and relations illustrated for KZ868 in Figure 26.6 are typical for the other drill holes. Disseminated ores occur in picritic and taxitic units at the base of the ore-bearing intrusions. Sulphide-mineral aggregates occur as coarse-grained elliptical droplets in picritic rocks and as coarse-grained irregularly shaped, interstitial mineral aggregates in the taxitic rocks. Interstitial-sulphide minerals also occur as thin films along grain boundaries in both rock types. There is no increase in sulphide proportion downward, nor is there any suggestion that the coarse sulphide aggregates were settling or aggregating. The taxitic unit grades downward into a sulphide-poor, fine-grained chill zone. Massive-sulphide accumulations occur below the chilled base of the intrusion, overlain either by chilled rocks at the base of the intrusion or by a thin septum of contact-metamorphosed sedimentary rocks that separates the massive ore from the intrusion.

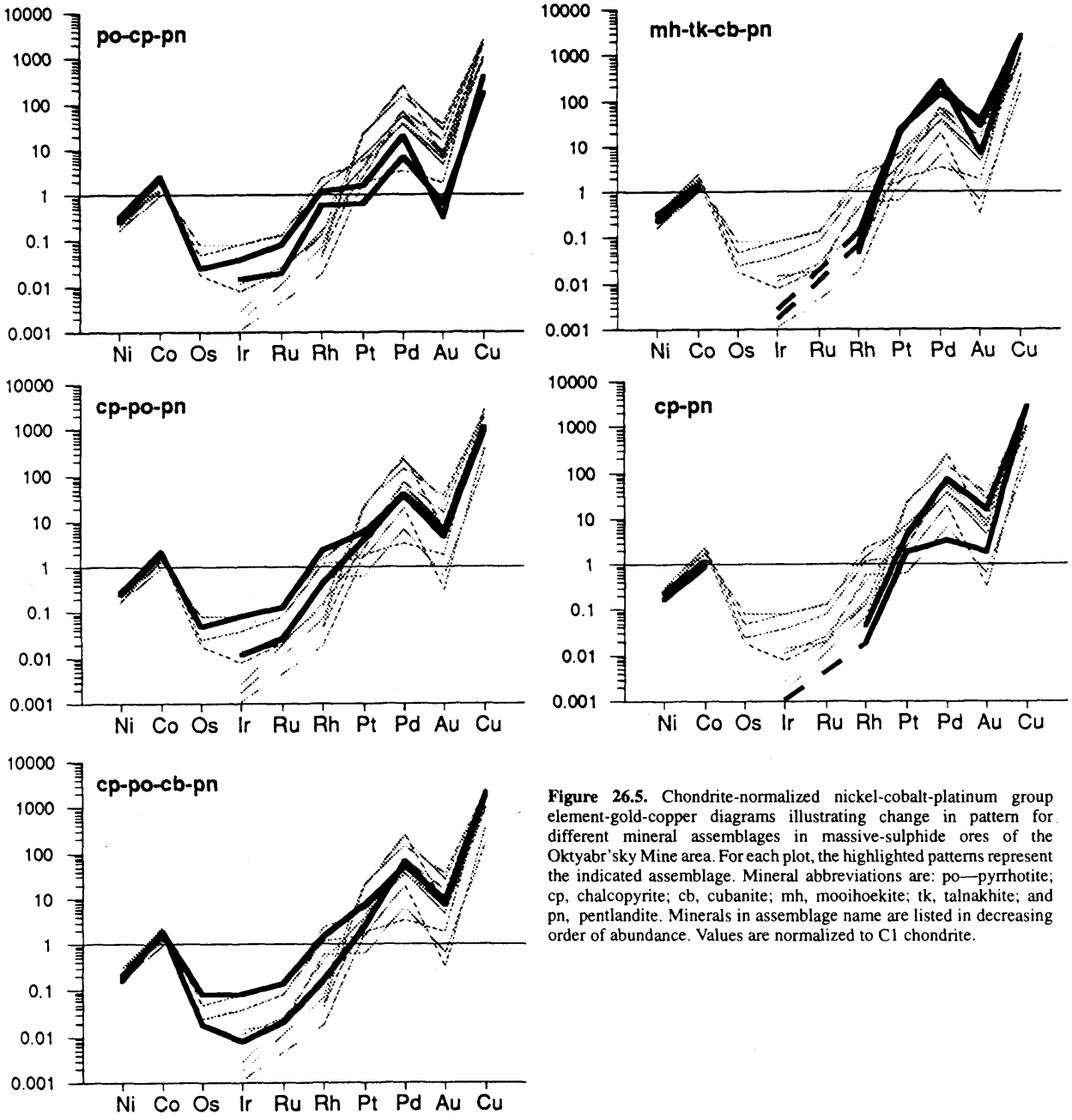


**Figure 26.5.** Chondrite-normalized nickel-cobalt-platinum group element-gold-copper diagrams illustrating change in pattern for different mineral assemblages in massive-sulphide ores of the Oktyabr'sky Mine area. For each plot, the highlighted patterns represent the indicated assemblage. Mineral abbreviations are: po—pyrrhotite; cp, chalcopyrite; cb, cubanite; mh, mooihoekite; tk, talnakhite; and pn, pentlandite. Minerals in assemblage name are listed in decreasing order of abundance. Values are normalized to C1 chondrite.

The compositions of spatially associated massive and disseminated ores recalculated to 100% sulphide for these drill holes are illustrated in Figures 26.7 and 26.8. Massive ores have lower platinum, palladium and gold concentrations than spatially associated disseminated ores. Less consistent relations are seen for iridium, ruthenium and rhodium; concentrations in massive ores can be higher, comparable, or lower than those in associated disseminated ore. These relations lead to characteristic shapes for the chondrite-normalized patterns; disseminated ores have patterns that have relatively smooth, positive slopes for the PGE (and low Pd/Pt ratios), whereas, the massive ores have high Pd/Pt ratios and patterns characterized by smooth positive slope from osmium to rhodium, a negative slope from rhodium to platinum and a positive slope from palladium to platinum. For descriptive purposes, the patterns typical of the massive ores are said to be characterized by negative platinum anomalies.

The differences between disseminated- and massive-ore compositions cannot be modelled by varying parameters in the equation that expresses partitioning of elements between sulphide and silicate liquids (Campbell and Naldrett 1979):

$$Y_i = X_i^o D_i \frac{(R + 1)}{(R + D_i)}$$

where $Y_i$ is the final concentration of element *i* in the sulphide liquid; $X_i^o$ is the initial concentration of element *i* in the silicate liquid; $D_i$ is the distribution coefficient of element *i* between sulphide liquid and silicate liquid; and R is the mass ratio of silicate liquid to sulphide liquid. The most obvious parameter to change is R; lower concentrations of PGE in massive ores relative to disseminated ores are generally thought to reflect lower values of R for the massive ores. If disseminated and massive ores are constrained to be derived from silicate magmas of similar composition ($X_i^o$), the higher Pd/Pt ratios observed in the massive ores cannot be obtained by varying R because, in order to do so, $D_{Pt}$ would have to be greater than $D_{Pd}$ because:

$$\frac{Y_{Pd}}{Y_{Pt}} = \frac{D_{Pd} X^o_{Pd} (R + D_{Pt})}{D_{Pt} X^o_{Pt} (R + D_{Pd})}$$

For $Y_{Pd}/Y_{Pt}$ to increase with decreasing R, $D_{Pt}$ must be greater than $D_{Pd}$. Studies of offset PGE patterns on the Great Dyke (Naldrett and Wilson 1990) and the Munni Munni Complex (Barnes et al. 1990) have demonstrated that $D_{Pd}$ must be greater than $D_{Pt}$. In addition, the Pd/Pt ratio of the silicate magma would have to be unreasonably high (greater than 7) to achieve the observed concentrations of PGE in the sulphide ores.

The compositions of the massive-sulphide ores cannot be modelled using liquid-liquid partitioning because some of the massive-sulphide ores do not represent liquid compositions. As illustrated in Figure 26.9, the composition of the massive ores in drill hole KZ1713 are nearly identical to the composition of MSS that would crystallize from a parental sulphide liquid that is approximated by the composition of the disseminated sulphides in the overlying taxitic and picritic units. These massive ores do not represent liquid

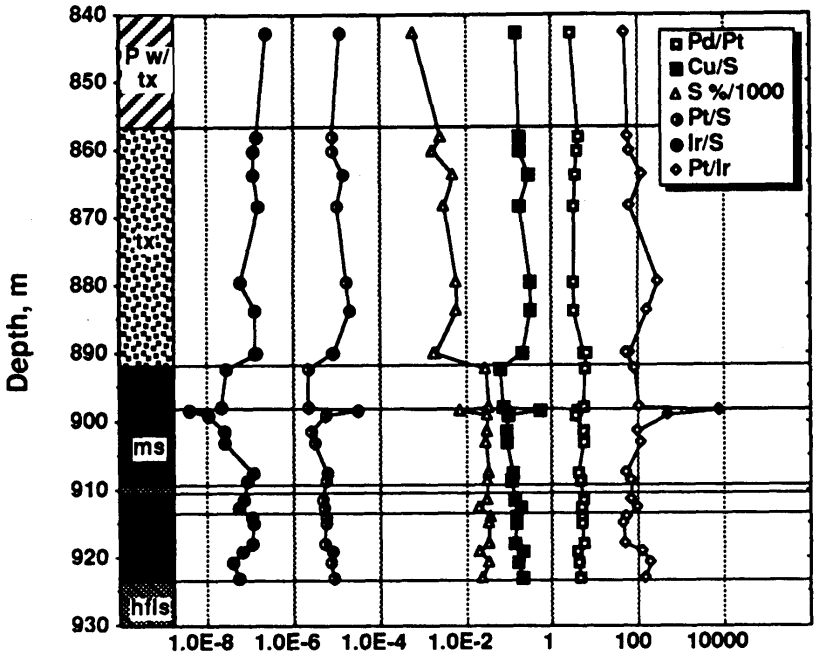


**Figure 26.6.** Lithologic column and stratigraphic variation of Pd/Pt, Cu/S, S, Pt/S, Ir/S and Pt/Ir for part of hole KZ868, Oktyabr'sky Mine area, Kharayelakh intrusion. Lithologic abbreviations are: p w/ tx—picrite with inclusions of taxitic rock; tx—taxitic gabbrodolerite; ms—massive sulphide; and hfls—contact-metamorphosed sedimentary rocks.

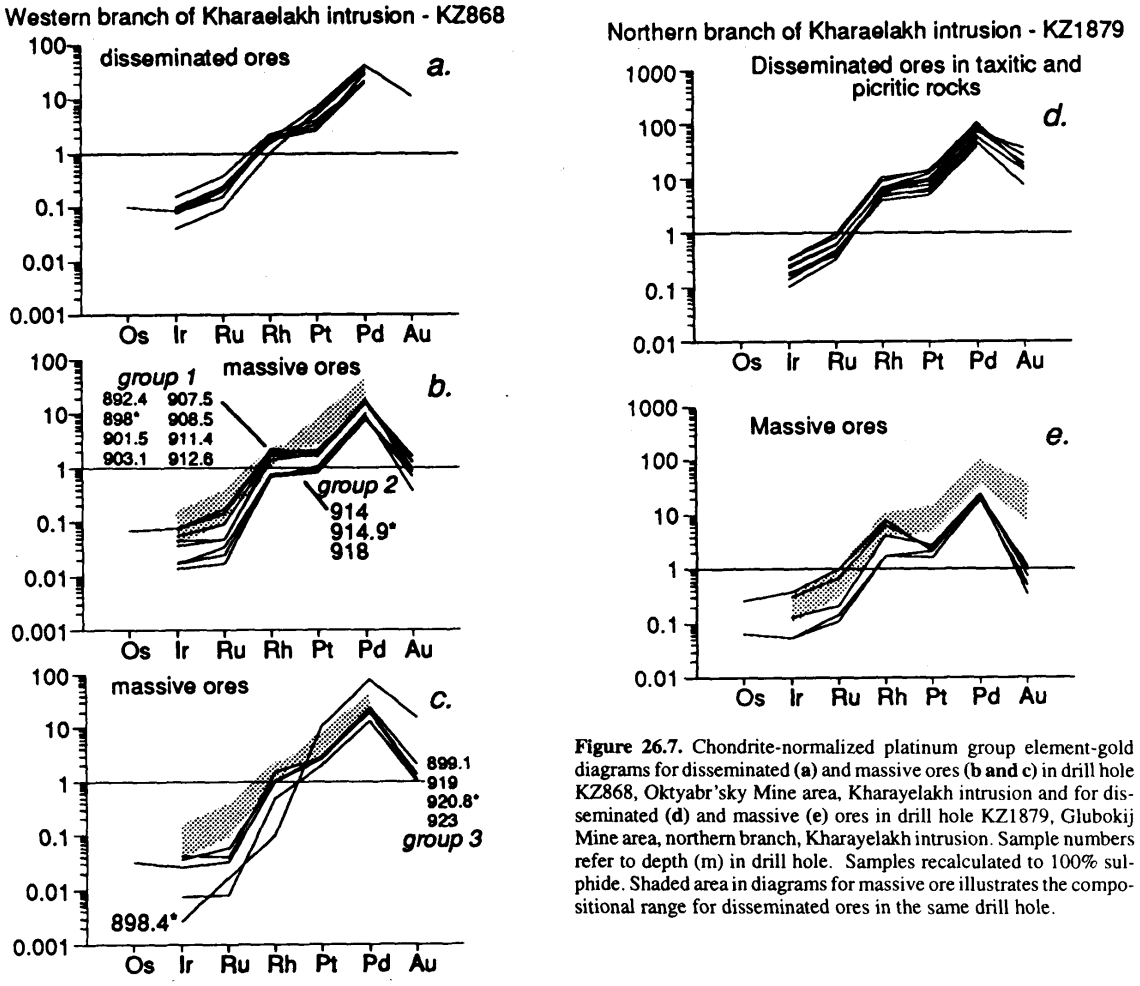


**Figure 26.7.** Chondrite-normalized platinum group element-gold diagrams for disseminated (**a**) and massive ores (**b and c**) in drill hole KZ868, Oktyabr'sky Mine area, Kharayelakh intrusion and for disseminated (**d**) and massive (**e**) ores in drill hole KZ1879, Glubokij Mine area, northern branch, Kharayelakh intrusion. Sample numbers refer to depth (m) in drill hole. Samples recalculated to 100% sulphide. Shaded area in diagrams for massive ore illustrates the compositional range for disseminated ores in the same drill hole.

compositions but are cumulates—some mixture of early precipitating MSS and trapped sulphide liquid. Partition coefficients ($D^{MSS/sulphide\ liquid}$) used to calculate MSS composition are the experimental values presented by Fleet et al. (1992) and reported orally in 1992: osmium, 5.3; iridium, 2.1; ruthenium, 3.2; rhodium, 3.1; platinum, 0.17; palladium, 0.14 and gold, 0.09.

The partition coefficients ($D^{MSS/sulphide\ liquid}$) for osmium, iridium, ruthenium and rhodium are all greater than 1 and for platinum, palladium and gold are less than 1; accordingly, one might anticipate that the osmium, iridium, ruthenium and rhodium contents in MSS cumulates would be greater than those in the parental-sulphide liquid and the platinum, palladium and gold contents would be less. The negative platinum anomaly that is typical of pyrrhotite-rich massive ores is not due to the depletion of platinum relative to the other PGE but reflects the difference in the distribution coefficients from osmium to rhodium and platinum to gold.

The massive ores in drill hole KZ1713 appear to represent a simple situation, where the cumulate is composed entirely of a cumulus phase of a composition that would crystallize from a parental liquid that is comparable to disseminated sulphides in the overlying intrusion. Although massive ores from KZ1799, KZ1879 and KZ868 have PGE patterns indicating that they are MSS cumulates, the compositions of disseminated ores associated with the massive-sulphide ores are not reasonable models for parental-sulphide-liquid compositions because the massive-sulphide ores have iridium, ruthenium and rhodium contents that are less than those in the associated disseminated ores. If osmium, iridium, ruthenium and rhodium are enriched in MSS relative to the liquids from which it crystallizes, the parental liquids for the massive-sulphide ores must be more fractionated (have lower concentrations of osmium, iridium, ruthenium and rhodium) than the sulphide liquids that crystallized to form the disseminated ores in the taxitic and picritic units. This points to a problem that is endemic in the study of cumulate processes: the difficulty in clearly identifying parental liquids from which cumulates are derived. The disseminated and massive ores are associated only by proximity; they are not physically interrelated. If the parental liquids for the

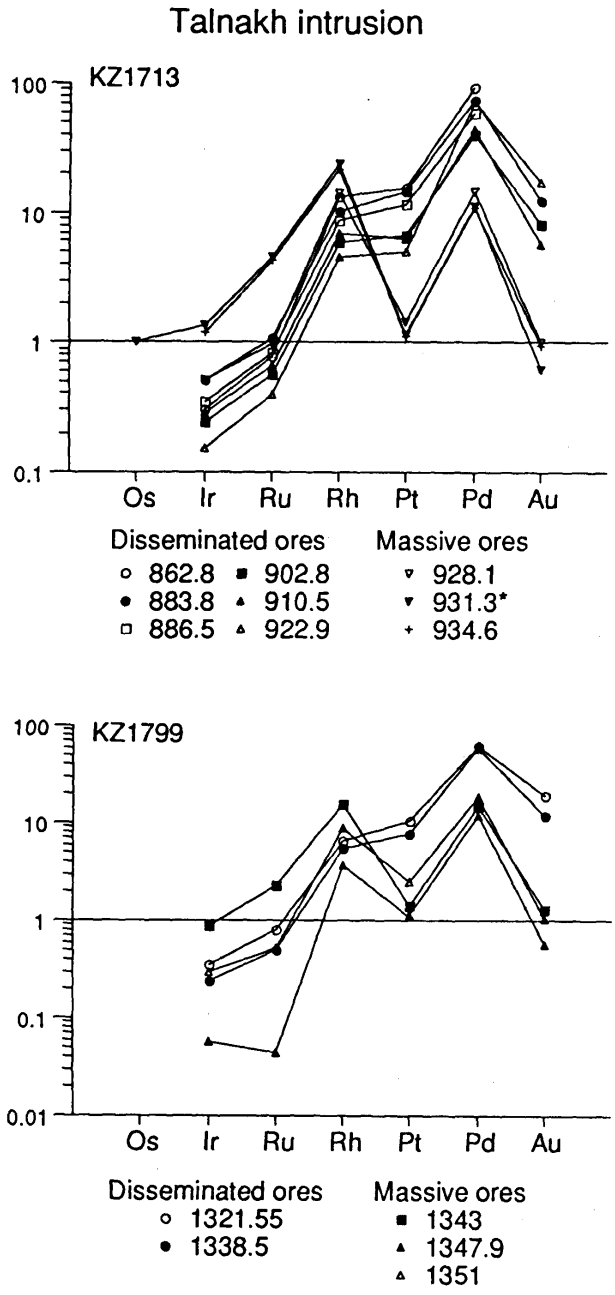


**Figure 26.8.** Chondrite-normalized platinum group element-gold diagrams for disseminated and massive ores in drill holes KZ1713 and KZ1799, Skalisty Mine area, Talnakh intrusion. Sample numbers refer to depth (m) in drill hole. Samples are recalculated to 100% sulphide.

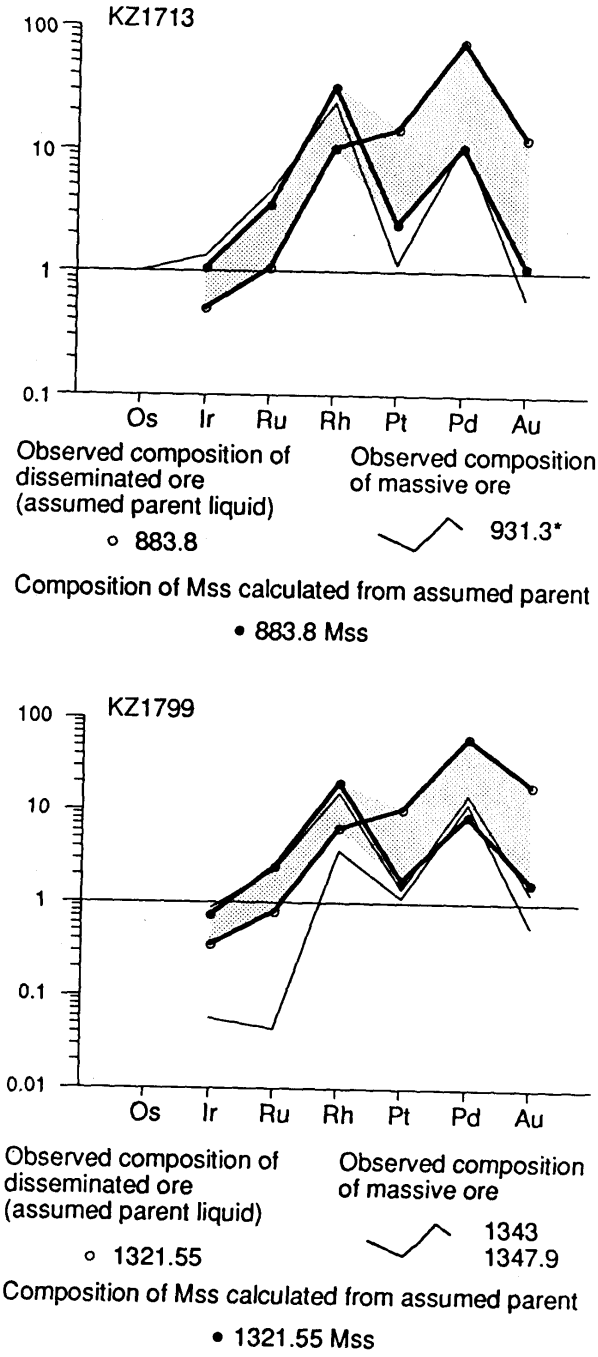


**Figure 26.9.** Chondrite-normalized platinum group element-gold diagrams for disseminated and massive ores in drill holes KZ1713 and KZ1799 compared to calculated composition of monosulphide solid solution (MSS; as described in text). Sample numbers refer to depth (m) in drill hole. Samples are recalculated to 100% sulphide. Shaded areas represent the compositional space between parent liquid (disseminated ores) and calculated composition of MSS. Thin lines represent the actual composition of massive-sulphide ore samples.

disseminated and massive ores are related, as suggested by lead isotope analyses (Wooden et al. 1992), either: 1) liquid parental to the massive ores previously fractionated MSS; or 2) it equilibrated under different conditions; or 3) there is a cumulate aspect to the disseminated ores as well (note the subtle negative platinum anomaly for the disseminated-ore compositions).

From studies of cumulate silicate rocks in layered mafic intrusions, it is well known that there are many processes that can affect the formation and development of cumulates; many of these are listed by Irvine (1987). More detailed analysis of the data from KZ868 indicate that many of the problems inherent with understanding the petrogenesis of silicate cumulates are also applicable to these sulphide cumulates.

Compositional trends for incompatible *versus* compatible elements in the massive-sulphide accumulation in KZ868 are inconsistent with *in situ* fractional crystallization of MSS from a single batch of sulphide liquid. Concentration of copper, platinum and palladium increases systematically toward the bottom of the massive-sulphide unit (*see* Figure 26.6). Although not illustrated in Figure 26.6, the concentration of iron shows a progressive decrease from the top to the bottom of the massive-sulphide unit. Assuming that iron is behaving in a compatible fashion by partitioning into MSS and copper, platinum and palladium are behaving as incompatible elements, the systematic compositional trends simply appear to indicate an increase in the trapped liquid component towards the base of the massive-sulphide unit. However, compositional trends for other elements that behave compatibly during MSS fractionation (iridium, ruthenium, rhodium) are not consistent with simply mixing MSS and trapped liquid. The compositional trends for iridium, ruthenium and rhodium do not vary antithetically with the incompatible elements but show a complex downhole distribution. The pattern appears to indicate that the progressive change in trapped liquid content is superimposed on several discrete intervals in which the original MSS appears to have had very different trace element compositions. These intervals may be separated by abrupt compositional discontinuities. This difference in behavior is also illustrated in Figure 26.10, where variation diagrams for platinum and palladium *versus* copper display positive linear trends, and data for rhodium and ruthenium *versus* copper appear to be scattered but actually consist of clusters of samples that may show positive correlations of iridium, ruthenium and rhodium with copper. This complexity indicated by the compostional trends for iridium, ruthenium and rhodium is also apparent in the chondrite-normalized PGE-gold diagrams for the massive ores (*see* Figure 26.7). The interval from 914 to 918 (group 2) is characterized by discretely lower PGE concentrations than overlying samples (group 1). Samples 899.1, 919, 920.8 and 923 (group 3) clearly show the affect of the addition of incompatible-enriched sulphide liquids (analogous to sample 898.4, a copper-rich sulphide segregation in a hornfels xenolith) to MSS cumulate; the patterns show only subtle negative platinum anomalies.

The complex relations suggested by inspection of the chondrite-normalized plots and covariation plots can be further investigated by constructing a simple model based upon the Rayleigh-distillation law. This relation can be used to model the distribution of trace elements between a liquid and solid during perfect (simple) fractional crystallization; the bulk-partition coefficients of elements between crystallizing minerals and liquid are assumed to be constant. Li et al. (1993) and Naldrett et al. (this volume) have used this relation to model the compositional affects of the fractional crystallization of sulphide liquids. This relation can be expressed as: $C_1^i = C_{o,1}^i f(D^i - 1)$ where $D^i$ is the bulk-partition coefficient (in this case the partition coefficient of element i between Mss and sulphide liquid);

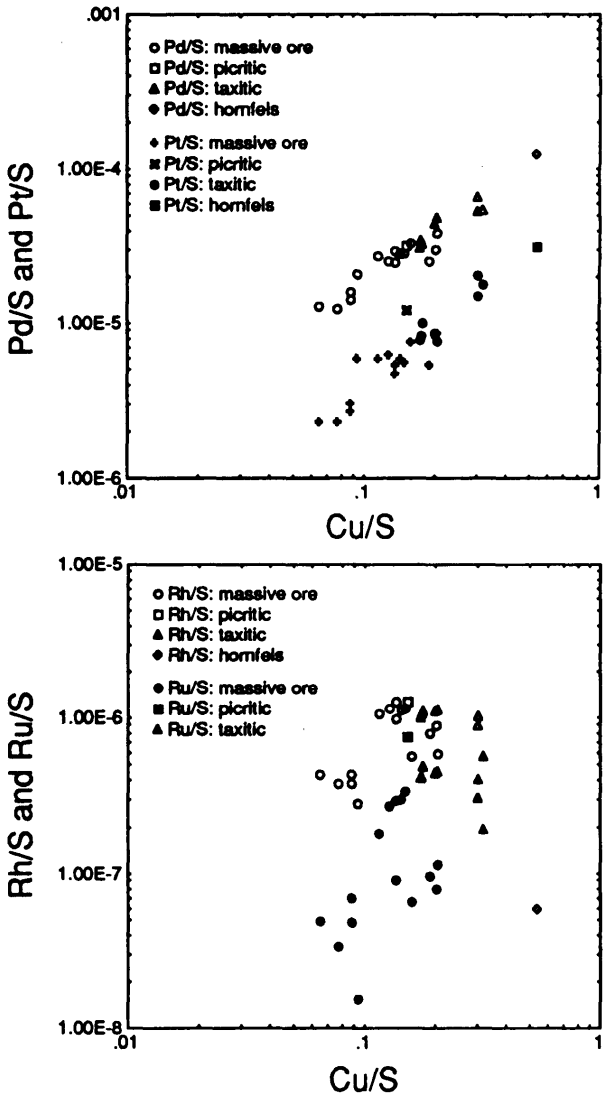


**Figure 26.10.** Variation diagrams for Pt/S and Pd/S *versus* Cu/S and Rh/S and Ru/S *versus* Cu/S for disseminated- and massive-ore types in drill hole KZ868, Oktyabr'sky Mine area, Kharayelakh intrusion.

$f$ is the weight proportion of residual liquid; $C^i_{o,l}$ is the concentration of element $i$ in the parental liquid; and $C^i_l$ is the concentration of element $i$ in the liquid (Allegre and Minster 1978). The concentration of trace elements in the instantaneous solid (in this case MSS) is: $C^i_{Mss} = D^i C^i_{o,1} f (D^i - 1)$.

The pyrrhotite-rich massive-sulphide ores below the base of the intrusion were assumed to be derived from parental liquids with elemental concentrations similar to samples of disseminated ores in taxitic rocks when recalculated to concentrations in 100% sulphide: copper, 7.0 weight %, platinum, 3500 ppb, palladium, 15 000 ppb, rhodium, 400 ppb and ruthenium, 160 ppb. Given this assumption and using the partition coefficients experimentally determined by Fleet et al. (1992 and listed above), the model calculated from the Rayleigh fractionation equations was not consistent with the data. However, qualitative constraints on the relative partition coefficients among elements, based on the slope of lines on element-element plots (which are dependent on the ratios of the partition coefficients), suggest that the D values should be modified. Slopes on element-element plots indicate that $D^{MSS/liquid}$ for copper is greater than for palladium which is greater than for platinum and that $D^{MSS/liquid}$ for ruthenium is greater than for rhodium. Values of $D^{MSS/liquid}$ used for the model are: copper, 0.1; palladium, 0.075; platinum, 0.05; ruthenium, 5.0 and rhodium, 3.0.

As deduced by inspection of the chondrite-normalized PGE patterns, comparison of model results and the data for KZ868 indicate that the pyrrhotite-rich massive-sulphide ores are not cumulates derived from parental liquids similar in composition to the disseminated ores in the taxitic gabbrodolerites (Figure 26.11). Massive ore compositions can only be modelled by MSS crystallization from liquids that are fractionated relative to the assumed, parental-liquid compositions; some samples from groups 1 and 3 require parental liquids that correspond to fractionated liquids with $f$ values as low as 0.3 to 0.4. The amount of trapped liquid varies from samples of groups 1 and 3 (close to the line defining $C_{MSS}$) with low amounts of trapped liquid (15 to 25%) to samples from group 2 (close to the $C_{liquid}$ line) with large amounts of trapped liquid (approximately 80%). On the ruthenium-copper diagram of Figure 26.11, the compositional data for sample groups 2 and 3 form discrete linear arrays that cross tie lines and suggest mixing of cumulus MSS crystallized from compositionally distinct batches of

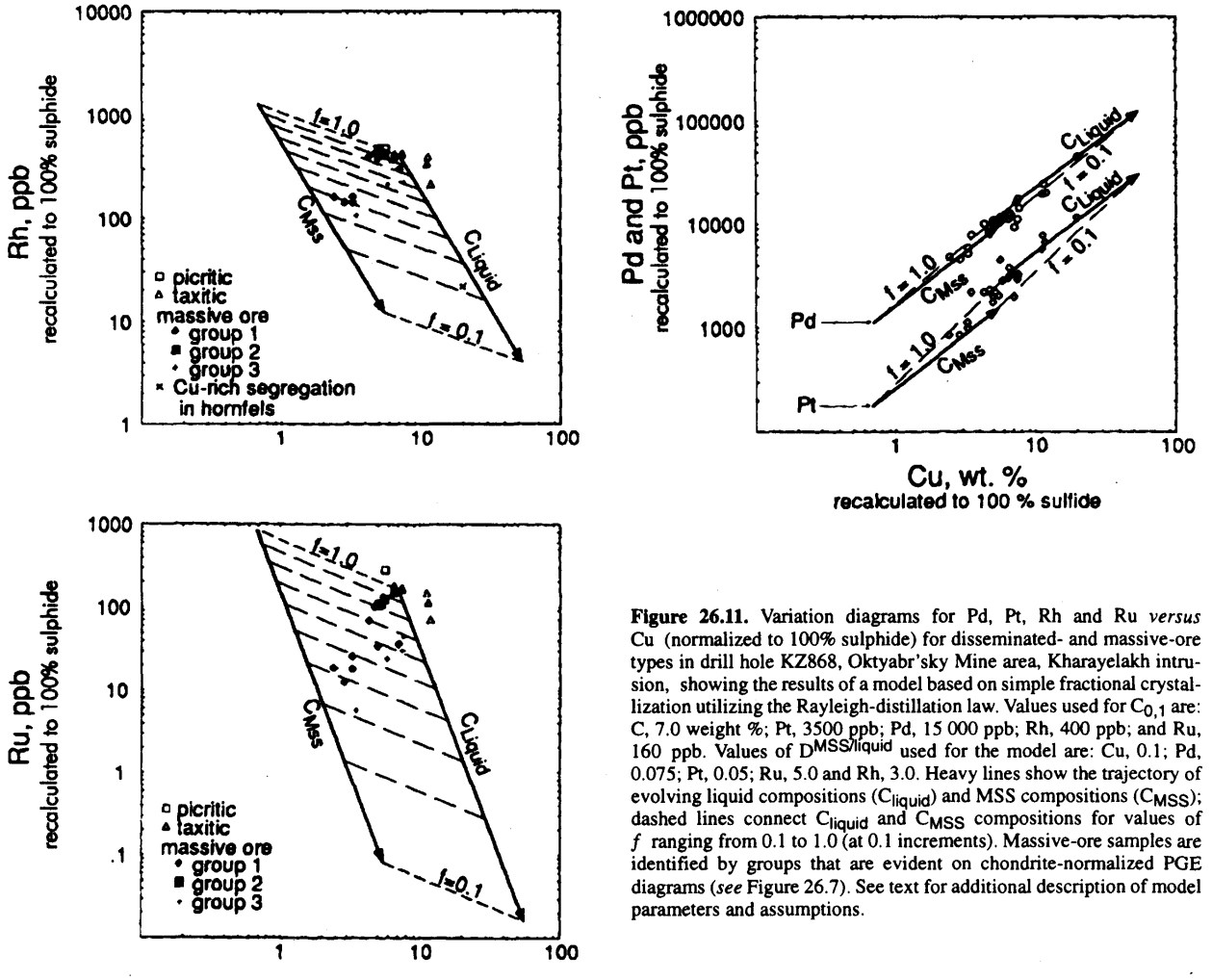


**Figure 26.11.** Variation diagrams for Pd, Pt, Rh and Ru *versus* Cu (normalized to 100% sulphide) for disseminated- and massive-ore types in drill hole KZ868, Oktyabr'sky Mine area, Kharayelakh intrusion, showing the results of a model based on simple fractional crystallization utilizing the Rayleigh-distillation law. Values used for $C_{0,1}$ are: C, 7.0 weight %; Pt, 3500 ppb; Pd, 15 000 ppb; Rh, 400 ppb; and Ru, 160 ppb. Values of $D^{MSS/liquid}$ used for the model are: Cu, 0.1; Pd, 0.075; Pt, 0.05; Ru, 5.0 and Rh, 3.0. Heavy lines show the trajectory of evolving liquid compositions ($C_{liquid}$) and MSS compositions ($C_{MSS}$); dashed lines connect $C_{liquid}$ and $C_{MSS}$ compositions for values of $f$ ranging from 0.1 to 1.0 (at 0.1 increments). Massive-ore samples are identified by groups that are evident on chondrite-normalized PGE diagrams (*see* Figure 26.7). See text for additional description of model parameters and assumptions.

fractionated parental liquid with less fractionated intercumulus liquid of perhaps 2 different compositions. Note also that the composition of the copper-rich segregation in hornfels plots near the $C_{liquid}$ line at an $f$ value close to 0.2. Model results for platinum, palladium and copper are also illustrated in Figure 26.11; the data are generally consistent with the model calculations with most samples falling within the parallelogram defined by the lines illustrating the composition of $C_{liquid}$ and $C_{MSS}$ and the tie lines for $f$ equal to 1.0 and 0.1. Samples of disseminated ore and the copper-rich segregation in hornfels plot near the liquid evolution line; massive-sulphide ores plot within the parallelogram. The similarity of partition coefficients do not allow a more quantitative discussion.

The data obtained for drill hole KZ868 suggest that MSS in the sampled, mineralized intercept has crystallized from a range of sulphide liquid compositions, that many samples represent a mixture of cumulus MSS and trapped liquid and that the interstitial melts may not be the liquids from which the MSS crystallized. As noted earlier, drill hole KZ868 is situated on the southern margin of the main Kharayelakh orebody and an adjacent orebody in the Tamyr Mine, which together consist of pyrrhotite-dominant ores characterized by simple zoning that grades westward into the complexly zoned ores of the Oktyabr'sky Mine area (*see* Figures 26.2 and 26.3). This zonation appears to record the lateral migration of copper-rich fractionated liquids during solidification of the orebody. The pyrrhotite-rich, sulphide cumulates in drill hole KZ868 record MSS crystallization from related but compositionally distinct sulphide liquids and suggest that lateral migration of liquids was episodic and complex. At least some of the cumulates could be derived from liquids that are only slightly fractionated relative to the composition of disseminated ores. The fractionated liquid compositions suggested by cumulates in groups 1 and 3 are similar to the compositions determined for chalcopyrite-pyrrhotite massive ores to the north of drill hole KZ868 (sample OC4 in Table 26.1). The systematic changes in copper content with depth in the hole and the apparent mixing trends in Figure 26.11 indicate that migration of interstitial melts through the MSS cumulates also plays an important role in determining the final composition of the ores.

If the massive sulphides in drill holes KZ1713, KZ1799 and KZ1879 are also cumulates, where are the copper- and PGE-enriched residual liquids? For KZ868, the residual liquid is obviously represented by the copper-rich ores to the north of the drill hole. The massive-sulphide intercepts in drill holes KZ1713 and KZ1799 are within one of a string of economic massive-sulphide orebodies that lie along the axis of the Talnakh intrusion. These massive-sulphide bodies probably form a single, large, interconnected ore system. The extent of the massive sulphides shown in Figure 26.2 are determined by economic considerations; in reality, they are connected by thin, but uneconomic, massive-sulphide units. Ores rich in copper from the Komsomolsky Mine area, east of the Noril'sk–Kharayelakh fault, may be residua from the cumulates we analyzed from the Skalisty Mine area. Our knowledge of the geometry of intrusions and distribution of ore in the northern branch of the Kharayelakh intrusion is limited; however, there are a number of copper-rich orebodies on the west side of the Noril'sk–Kharayelakh fault that could be part of the compositionally zoned ore system that would include the massive sulphide in drill hole KZ1879.

# DISCUSSION

Fractional crystallization of sulphide liquids is not a new concept. It was initially proposed by Hawley (1962, 1965) to explain the mineralogical and compositional zonation of magmatic ore deposits at Sudbury. Subsequent experimental investigations of sulphide systems have supported the hypothesis that copper-rich residual liquids could be derived by fractional crystallization (Craig and Kullerud 1969; Hill 1984; Makovicky et al. 1986). Compositional zonation or differentiation resulting from fractional crystallization and progressive removal of copper-rich liquids from early crystallizing MSS have been suggested for ores of the Sudbury district (Keays and Crocket 1970; Chyi and Crocket 1976; Cabri and LaFlamme 1976; Naldrett et al. 1982; and Li et al. 1992), as well as ores associated with the Insizwa Complex (Lightfoot et al. 1984), the Talnakh intrusion (Genkin et al. 1982) and komatiite-hosted nickel deposits (Barnes and Naldrett 1987). Emphasis has been placed on the residua resulting from the fractionation process in order to explain the presence of paragenetically late copper-rich ores commonly associated with magmatic sulphide deposits. The concentration of PGE into the residua was a principal area of interest because the residua are enriched in precious metals and the qualitative behavior of PGE during sulphide-liquid fractionation can be determined (limitations of instrumental analysis prohibited the experimental determination of partitioning behavior). The summary data for samples of the compositionally zoned orebody of the Oktyabr'sky Mine are consistent with the experimental determinations for MSS fractionation from a sulphide liquid and provide qualitative information for the partitioning behavior for a large suite of elements associated with magmatic sulphide systems.

Compositional differences between massive, matrix and disseminated ores within individual deposits have also been attributed to fractional crystallization. Lightfoot et al. (1984) noted that differences in rhodium, ruthenium, iridium, osmium, nickel and copper between disseminated and massive ores in the Insizwa Complex are consistent with MSS fractionation, but that platinum and palladium were not as enriched in certain massive ore types as might be expected. In considering compositional variation in ore types at Alexo, Barnes and Naldrett (1986) showed that the iridium-rich massive sulphides and the palladium-rich matrix sulphides could be derived by crystal fractionation of MSS from a sulphide liquid with a composition similar to that of the disseminated sulphides. The iridium-enriched sulphides represent MSS cumulates, and the palladium-enriched sulphides represent fractionated liquids (Figure 26.12).

Barnes et al. (1988) observed compositional differences between massive and matrix ores at Agnew similar to those observed at Alexo by Barnes and Naldrett (1986).

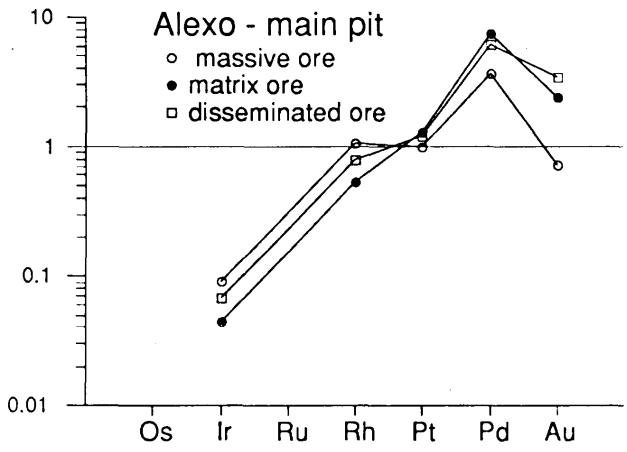


**Figure 26.12.** Chondrite-normalized platinum group element-gold diagrams for disseminated, matrix and massive ores from the Alexo main pit (Barnes and Naldrett 1987). Samples are recalculated to 100% sulphide.

They rejected *in situ* differentiation of sulphide liquids as a possible explanation for the difference in composition because massive ores overlie the flow which hosts the matrix ore. The ores are spatially associated but not physically related, much like the ores at Noril'sk–Talnakh. The compositional differences could not simply be attributed to variations in R (mass ratio of silicate to sulphide liquid) because osmium, iridium, ruthenium and rhodium are enriched in the massive ores, whereas platinum, palladium and gold are depleted. Variations in R would have affected all the PGE in a similar manner because they have similar $D^{(sulphide/silicate)}$. A strong negative platinum anomaly is also characteristic of the normalized PGE patterns. Barnes et al. (1988) suggested that different ore types formed from different batches of sulphide liquid, which separated under different temperatures or fugacities ($f$) of sulfur and/or oxygen. They note that the partition coefficient for any PGE into sulphide liquid becomes strongly dependent on $f_{S2}$ below its sulfidation curve. They propose that massive-ore sulphides segregated at conditions above the osmium and iridium sulfidation curves; whereas, matrix ores segregated below the sulfidation curves for these elements. The matrix ores would contain less osmium and iridium because these elements are partitioned less efficiently into the sulphide-liquid phase because of the presence of coexisting PGE alloys. They suggested that the negative platinum anomalies characteristic of the massive ores may result from a similar process (partitioning being affected by platinum alloy coexisting with sulphide liquid). The lower platinum, palladium and nickel contents of the massive ores were thought to reflect batch equilibration in a local sulphide-rich environment giving rise to a low magma-sulphide ratio.

Compositional differences between massive and matrix ores has also been attributed to hydrothermal or metamorphic redistribution. For deposits in Western Australia, Ross and Keays (1979), Keays et al. (1981) and Cowden et al. (1986) suggested that lower palladium concentrations in massive-sulphide ores can be attributed to loss of palladium to copper-rich veins that form during metamorphism. Barnes et al. (1985) noted negative platinum anomalies in ores associated with komatiites in Western Australia and the Abitibi belt in Canada and suggested that both gold and platinum were remobilized from these ores by metamorphism and later talc-carbonate alteration.

Massive-sulphide ores associated with many magmatic-sulphide deposits share common compositional features regardless of the environment of formation and the subsequent metamorphic or alteration history. Chondrite- or mantle-normalized PGE patterns of massive ores commonly are characterized by negative platinum anomalies (Figure 26.13). Massive ores can contain higher proportions of pyrrhotite than disseminated- or matrix-sulphide ores. Only in some examples do the massive-sulphide ores contain more osmium, iridium, ruthenium and rhodium and less platinum, palladium and gold relative to disseminated and matrix ores. As illustrated earlier, any number of *ad hoc* hypotheses can be proposed to explain the peculiarities of a given deposit; however, the recurrence of similar compositional features indicate that there must be a common, fundamental geological process involved.

Our analysis of the field relations and compositional data for the Noril'sk–Talnakh area suggests that the compositional similarities result from cumulus processes. As indicated earlier, many previous studies of fractional-crystallization processes have focussed on the residua generated by the process; little emphasis has been placed on the complementary sulphide cumulates. Sulphide cumulates can be recognized by their distinct compositional characteristics. The complexity of cumulus processes implies that sulphide cumulates can occur in a multitude of geological situations. Difficulties in relating spatially associated massive and disseminated ores do not negate the role of cumulate processes in determining the composition of the massive ores but reflect our assumption that disseminated-ore compositions can be used as a model for the parental-sulphide liquids.

## ACKNOWLEDGMENTS

We would like to thank all the geologists from TsNIGRE who made the arrangements for and facilitated our visit to the Noril'sk–Talnakh area; in particular, we recognize Igor Migachev and Alexi Volchkov. We also wish to extend our thanks to personnel with the Noril'sk combine and the Noril'sk Expedition for their hospitality at the time of our visit and their continued support of this project. We thank those who have provided analytical data from within the U.S. Geological Survey: P.H. Briggs, R.R. Carlson, Neil Elsheimer, T.L. Fries, P.J. Lamothe, A.L. Meier and Sarah Prebble. We acknowledge many insightful discussions with J.L. Wooden and G.K. Czamanske of the U.S. Geological Survey. Reviews by D.C. Peck, Peter Lightfoot, and George Albino substantially improved the manuscript.

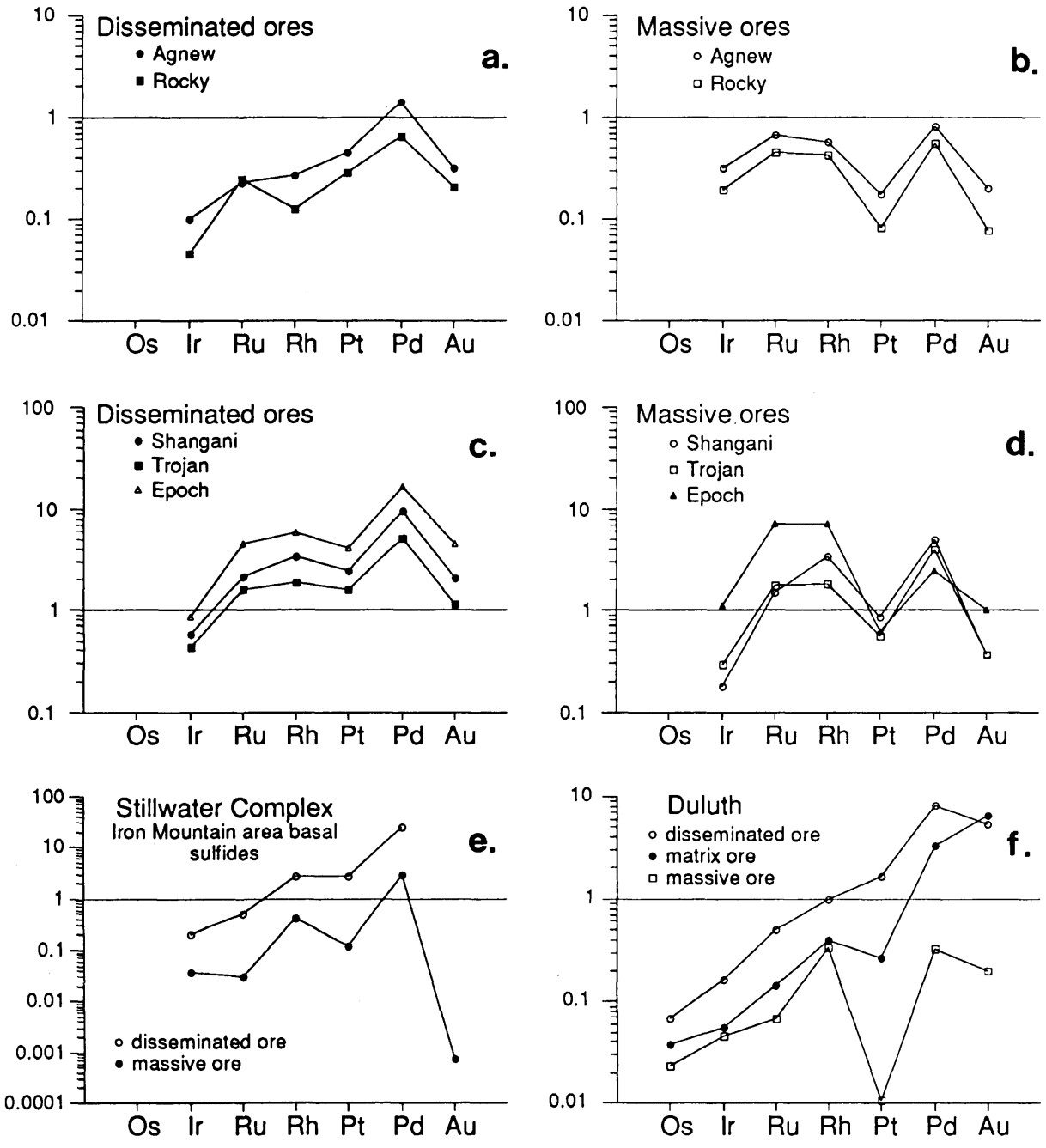


**Figure 26.13.** Chondrite-normalized platinum group element-gold diagrams for magmatic sulphide deposits in which massive ores are compositionally distinct from disseminated and matrix ores. Note that the massive ore types are characterized by negative platinum anomalies. **a)** and **b)** Komatiite- associated disseminated and massive ores from Agnew and Rocky's Reward, Western Australia (Barnes et al. 1988). **c)** and **d)** Komatiite-associated disseminated and massive ores from Shangani, Trojan and Epoch, Zimbabwe (Naldrett 1981). **e)** Sulphide mineralization near the base of the Stillwater Complex in the Iron Mountain area and **d)** sulphide mineralization near the base of the Duluth Complex, Babbitt deposit (Ripley 1990). Patterns represent averages of reported analyses; samples were recalculated to 100% sulphide.

# REFERENCES


Allegre, C.J. and Minster, J.F. 1978. Quantitative models of trace element behavior in magmatic processes; Earth and Planetary Science Letters, v.38, p.1–25.

Aruscavage, P.J. and Crock, J.G. 1987. Atomic absorption methods; *in* Methods for Geochemical Analysis, United States Geological Survey, Bulletin 1770, p.C1–C6.

Barnes, S.J., Gole, M.J. and Hill, R.E.T. 1988. The Agnew Nickel Deposit, Western Australia: part II. Sulfide geochemistry, with emphasis on the platinum-group elements; Economic Geology, v.83, no.3, p.537–550.

Barnes, S.J., McIntyre, J.R., Nisbet, B.W. and Williams, C.R. 1990. Platinum group element mineralization in the Munni Munni Complex, Western Australia; Mineralogy and Petrology, v.42, p.141–164.

Barnes, S.-J. and Naldrett, A.J. 1986. Variation in platinum group elements concentrations in the Alexo mine komatiite, Abitibi greenstone belt, northern Ontario; Geological Magazine, v.123, p.515–524.

——1987. Fractionation of the platinum-group elements and gold in some komatiites of the Abitibi greenstone belt, northern Ontario; Economic Geology, v.82, p.165–183.

Barnes, S.-J., Naldrett, A.J., Gorton, M.P. 1985. The origin of the fractionation of platinum-group elements in terrestrial magmas; Chemical Geology, v.53, p.303–323.

Cabri, L.J. and Laflamme, J.H.G. 1976. The mineralogy of the platinum-group elements from some copper-nickel deposits of the Sudbury area, Ontario; Economic Geology, v.71, p.1159–1195.

Campbell, I.H. and Naldrett, A.J. 1979. The influence of silicate:sulfide ratio on the geochemistry of magmatic sulfides; Economic Geology, v.74, p.1503–1505.

Chyi, L.L. and Crocket, J.H. 1976. Partition of platinum, palladium, iridium, and gold among coexisting minerals from the deep ore zone, Strathcona Mine, Sudbury, Ontario; Economic Geology, v.71, p.1196–1205.

Coombes, J.S. 1991. Platinum 1991; Johnson Matthey Public Limited Company, London, 64p.

Cowden, A., Donaldson, M.J., Naldrett, A.J. and Campbell, I.H. 1986. Platinum-group elements and gold in the komatiite-hosted Fe-Ni-Cu sulfide deposits at Kambalda, Western Australia; Economic Geology, v.81, p.1226–1235.

Craig, J.R. and Kullerud, G. 1969. Phase relations in the Cu-Fe-Ni-S system and their application to magmatic ore deposits; *in* Magmatic Ore Deposits, Economic Geology, Monograph 4, p.344–358.

Czamanske, G.K., Kunilov, V.E., Zientek, M.L., Cabri, L.J., Calk, L.C. and Likhachev, A.P. 1992. A proton-microprobe study of sulfide ores from the Noril'sk–Talnakh district, Siberia; Canadian Mineralogist, v.30, p.249–288.

DeYoung, J.H., Sutphin, D.M., Werner, A.B.T. and Foose, M.P. 1985. International strategic minerals inventory summary report-nickel; United States Geological Survey, Circular 930–D, 62p.

Distler, V.V., Maleshiy, A.,Yu and Laputina, I.P. 1977. Distribution of platinoids between pyrrhotite and pentlandite in crystallization of a sulfide melt; Geochemistry International, v.14, p.30–40.

Duzhikov, O.A., Distler, V.V., Strunin, B.M., Mkrtychyan, A.K., Sherman, M.L., Sluzhenikin, S.S. and Lurye, A.M. eds. 1992. Geology and metallogeny of sulfide deposits, Noril'sk region, U.S.S.R.; Society of Economic Geologists, Special Publication Number 1, 242p.

Fleet, M.E., Chryssoulis, S.L., Stone, W.E. and Weisener, C.G. 1992. Laboratory partitioning of precious metals between (Fe, Ni, Cu) monosulfide liquid and solid solution by SIMS and EMP; *in* Program with Abstracts, Geological Association of Canada–Mineralogical Association of Canada, v.17, p.A34.

Gary, M., McAfee, Jr., R. and Wolf, C.L. eds. 1972. Glossary of geology; American Geological Institute, Washington, D.C., 805p.

Genkin, A.D., Distler, V.V., Gladyshev, G.D., Filimonova, A.A., Evstigneeva, T.L., Kovalenker, V.A., Laputina, I.P., Smirnov, A.V. and Grokhovskaya, T.L. 1982. Copper-nickel sulphide ores of the Noril'sk deposits; Canada Centre for Mineral and Energy Technology, Mineral Research Program Mineral Sciences Laboratories Division, Report MRP/MSL 82–90, 446p.

Hawley, J.E. 1962. The Sudbury ores: their mineralogy and origin; Mineralogical Association of Canada, University of Toronto Press, Toronto, 207p.

——1965 Upside-down zoning at Frood, Sudbury, Ontario; Economic Geology, v.60, p.529–575.

Hill, R.E.T. 1984. Experimental study of phase relations at 600C in a portion of the Fe-Ni-Cu-S system and its application to natural sulphide assemblages; *in* Sulfide Deposits in Mafic and Ultramafic Rocks, The Institution of Mining and Metallurgy, p.14–21.

Hulbert, L.J., Duke, J.M., Eckstrand, O.R., Lydon, J.W., Scoates, R.F.J., Cabri, L.J. and Irvine, T.N. 1988. Geological environments of the platinum-group elements; Geological Survey of Canada, Open File 1440, 148p.

Irvine, T.N. 1987. Appendix II. Processes involved in the formation and development of layered igneous rocks; *in* Origins of Igneous Layering, D. Reidel Publishing Company, p.649–656.

Jackson, L.L., Brown, F.W. and Neil, S.T. 1987. Major and minor elements requiring individual determination, classical whole rock analysis, and rapid rock analysis; *in* Methods for Geochemical Analysis, United States Geological Survey, Bulletin 1770, p.G1–G23.

Jackson, S.E., Fryer, B.J., Gosse, W., Healy, D.C., Longerich, H.P. and Strong, D.F. 1990. Determination of the precious metals in geological materials by inductively coupled plasma-mass spectrometry (ICP-MS) with nickel sulfide fire-assay collection and tellurium coprecipitation; Chemical Geology, v.83, p.119–132.

Keays, R.R. and Crocket, J.H. 1970. A study of precious metals in the Sudbury nickel irruptive ores; Economic Geology, v.65, p.438–450.

Keays, R.R., Ross, J.R. and Woolrich, P. 1981. Precious metals in volcanic peridotite-associated nickel sulfide deposits in western Australia. II: Distribution within the ores and host rocks at Kambalda; Economic Geology, v.76, p.1645–1674.

Li, C., Naldrett, A.J., Coats, C.J.A. and Johannessen, P. 1992. Platinum, palladium, gold, and copper-rich stringers at the Strathcona Mine, Sudbury: Their enrichment by fractionation of sulfide liquid; Economic Geology, v.87, p.1584–1598.

Li, C., Naldrett, A.J., Rucklidge, J.C. and Kilius, L.R., 1993. Concentrations of platinum-group element and gold concentrations in sulfide minerals from the Strathcona deposit, Sudbury, Ontario; Canadian Mineralogist, v.31, pt.2, p.523–532.

Lichte, F.E., Golightly, D.W. and Lamothe, P.J. 1987. Inductively coupled plasma-atomic emission spectrometry; *in* Methods for Geochemical Analysis, United States Geological Survey, Bulletin 1770, p.B1–B10.

Lightfoot, P.C., Naldrett, A.J. and Hawkesworth, C.J. 1984. The geology and geochemistry of the Waterfall Gorge section of the Insizwa Complex with particular reference to the origin of the nickel sulfide deposits; Economic Geology, v.79, no.8, p.1857–1879.

Makovicky, M., Makovicky, E. and Rose Hansen, J. 1986. Experimental studies on the solubility and distribution of platinum-group elements in base-metal sulphides in platinum deposits; *in* Metallogeny of Basic and Ultrabasic Rocks, The Institution of Mining and Metallurgy, p.415–425.

Meier, A.L., Carlson, R.R. and Taggert, Jr., J.E. 1991. The determination of the platinum-group elements in geological materials by inductively coupled plasma mass spectrometry; *in* Programme and Abstracts, 6th International Platinum Symposium, July 8th-11th, 1991, Perth, Western Australia, p.38.

Milanovskiy, Ye, Ye 1976. Rift zones of the geological past and their associated formations, report 2; International Geology Review, v.18, p.619–639.

Naldrett, A.J. 1981. Nickel sulfide deposits: classification, composition, and genesis; *in* Economic Geology Seventy-Fifth Anniversary Volume, 1905–1980, Economic Geology Publishing Co., p.628–685.

——— 1989. Magmatic sulfide deposits; Oxford Monographs on Geology and Geophysics, no.14, Oxford University Press, New York, 186p.

Naldrett, A.J., Innes, D.G., Sowa, J and Gorton, M.P. 1982. Compositional variations within and between five Sudbury ore deposits; Economic Geology, v.77, p.1519–1534.

Naldrett, A.J. and Wilson, A.H. 1990. Horizontal and vertical variations in noble-metal distribution in the Great Dyke of Zimbabwe: A model for the origin of the PGE mineralization by fractional segregation of sulfide; Chemical Geology, v.88, p.279–300.

Ripley, E.M. 1990. Platinum-group element geochemistry of Cu-Ni mineralization in the Basal zone of the Babbitt deposit, Duluth Complex, Minnesota; Economic Geology, v.85, p.830–841.

Robert, R.V.D., van Wyk, E. and Palmer, R. 1971. Concentration of the noble metals by a fire-assay technique using NiS as the collector; National Institute of Metallurgy, Johannesburg, Report no.1371, 15p.

Ross, J.R. and Keays, R.R. 1979. The distribution of precious metals in the ores and host rocks at Kambalda, Western Australia; Canadian Mineralogist, v.17, p.417–435.

Smirnov, M.F. 1966. The structure of Noril'sk nickel-bearing intrusions and the genetic types of their sulfide ores; Moscow, Nedra, 58p. (in Russian).

Stekhin, A.I. 1992. Mineralogical and geological characteristics of the Talnakh ore junction (Abstract); Canadian Mineralogist, v.30, p.478.

Streckeisen, A.L. 1973. Plutonic rocks—Classification and nomenclature recommended by the IUGS Subcommission and the systematics of igneous rocks; Geotimes, v.18, no.10, p.26–30.

Strishkov, V.V. 1984. The copper industry of the U.S.S.R.: Problems, issues, and outlook; United States Bureau of Mines, Minerals Issues, 80p.

Wilson, S.A., Kane, J.S., Crock, J.G. and Hatfield, D.B. 1987. Chemical methods of separation for optical emission, atomic absorption spectrometry, and colorimetry; *in* Methods for Geochemical Analysis, United States Geological Survey, Bulletin 1770, p.D1–D14.

Wooden, J.L., Czamanske, G.K., Bouse, R.M., Likhachev, A.P., Kunilov, V.E. and Lyul'ko, V. 1992. Pb isotope data indicate a complex, mantle origin for the Noril'sk–Talnakh ores, Siberia; Economic Geology, v.87, p.1153–1165.

Wyllie, R.J.M. 1987. Platinum-production-projects-prospects; Engineering and Mining Journal, v.188, no.10, p.26–34.

Zientek, M.L., Fries, T.L. and Vian, R.W. 1990. As, Bi, Hg, S, Sb, Sn, and Te geochemistry of the J-M Reef, Stillwater Complex, Montana: Constraints on the origin of PGE-enriched sulfides in layered intrusions; Journal of Geochemical Exploration, v.37, p.51–73.

Zonenshain, L.P., Kuzmin, M.I. and Natapov, L.M. 1990. Geology of the USSR: A plate-tectonic synthesis; American Geophysical Union, Geodynamics Series, v.21, 242p.